Wind and Structures, *Vol. 32, No. 1 (2021) 31-46*
DOI: https://doi.org/10.12989/was.2021.32.1.31

Stability/instability of the graphene reinforced nano-sized shell employing modified couple stress model

Zhigang Yao*[1,2], Hui Xie[1] and Yulei Wang[3]

[1]*Department of Electronic and Optic Engineering, Army Engineering University, Shijiazhuang 050003, China*
[2]*School of Automation and Electrical Engineering, University of Science and Technology, Beijing 100083, China*
[3]*Institute of Electronics and Information Engineering, Tongji University, Shanghai 200082, Shanghai, China*

(*Received July 20, 2020, Revised January 2, 2021, Accepted January 15, 2021*)

Abstract. The current research deals with, stability/instability and cylindrical composite nano-scaled shell's resonance frequency filled by graphene nanoplatelets (GPLs) under various thermal conditions (linear and nonlinear thermal loadings). The piece-wise GPL-reinforced composites' material properties change through the orientation of cylindrical nano-sized shell's thickness as the temperature changes. Moreover, in order to model all layers' efficient material properties, nanomechanical model of Halpin-Tsai has been applied. A functionally modified couple stress model (FMCS) has been employed to simulate GPLRC nano-sized shell's size dependency. It is firstly investigated that reaching the relative frequency's percentage to 30% would lead to thermal buckling. The current study's originality is in considering the multifarious influences of GPLRC and thermal loading along with FMCS on GPLRC nano-scaled shell's resonance frequencies, relative frequency, dynamic deflection, and thermal buckling. Furthermore, Hamilton's principle is applied to achieve boundary conditions (BCs) and governing motion equations, while the mentioned equations are solved using an analytical approach. The outcomes reveal that a range of distributions in temperature and other mechanical and configurational characteristics have an essential contribution in GPLRC cylindrical nano-scaled shell's relative frequency change, resonance frequency, stability/instability, and dynamic deflection. The current study's outcomes are practical assumptions for materials science designing, nano-mechanical, and micro-mechanical systems such as micro-sized sensors and actuators.

Keywords: various thermal distributions; graphene nanoplatelet; resonance frequency; stability/instability; modified couple stress model

1. Introduction

Due to the last improvement in technology and science, composite reinforcement has attracted considerable attention (Gao *et al*. 2020, Gao, Wu *et al*. 2020, Hassanzadeh-Aghdam *et al*. 2018, Gao *et al*. 2018, Zhu *et al*. 2018, Gao *et al*. 2019, He *et al*. 2019, Liu *et al*. 2019, Gao *et al*. 2020, Li *et al*. 2020, Luo *et al*. 2020, Wang *et al*. 2020a, Wang *et al*. 2020b). There are a range of practical applications in GPL fillers which are presented in Ref (Shi *et al*. 2018). Moreover, the GPLs' mechanical characteristics making them a suitable selection in the usages of physics, chemistry, materials science, electrical engineering and nanosciences (Shi *et al*. 2018). Zhao *et al*. 2020) presented a review on the GPLs for their enhanced mechanical behaviors such as improved Young's modulus, which is exceptional along with high specific surface area, high strength, and a decent conductivity.

Rafiee *et al*. 2009 contrasted the epoxy's mechanical characteristics of nanocomposites enhanced by 1% fraction of multi-walled-carbon-nanotubes (MWNTs), single-walled-carbon-nanotubes (SWNTs) and each GPL. Their outcomes disclose that, GPLs' overall tensile strength, Young constant, resistance of fatigue, energy of fracture, and toughness of fracture are much higher than conventual materials. Thereby, GPL fillers can be used in many applications instead of highly-used MWNTs and SWNTs as reinforcements. Moreover, Yavari *et al*. 2010) presented epoxy/GPL nanocomposites' microstructure. Ref. (Bourada *et al*. 2020) analyzed SWCNTs' dynamic and stability investigations reinforcing a concrete beam lied on an elastic-substrate. In their work, the analytical solutions were derived through using energy methods and Navier approach for finding buckling and natural frequency information of the structure. Bousahla *et al*. 2020) studied dynamic and buckling characteristics of the simply supported SWCNTs reinforced beams using an integral-first-shear-deformation approach. Ref. (Alimirzaei *et al*. 2019) has scrutinized nonlinear viscoelastic-micro-composite-beams' vibration, buckling, and static investigations filled by multifarious boron nitride nanotube (BNNT) distributions with primary imperfect configuration via modified-strain-gradient model (MSG) through employing a finite element (FE) model. Medani *et al*. 2019) investigated dynamic and static characteristics of SWCNTs sandwich (PMPV) polymer plate with porosity via FSDT. Based on the FSDT dynamic and static characteristics of carbon-nanotube-composite filled sandwich plates via Hamilton's principle and analytical equations were presented by Ref. (Draoui *et al*. 2019). Researches demonstrated that subjoining highly

*Corresponding author, Ph.D.
E-mail: zhangsanfeng@gdou.edu.cn

ISSN: 1226-6116 (Print), 1598-6225 (Online)

graphene's negligible amount into initial matrix would enhance its thermal, mechanical and electrical behaviors. It would be worth mentioning that nano-scaled structures enhanced by GPLs are much more practical in designing of engineering applications. Therefore, a focus on GPLs reinforcing nanostructure would be highly suggested by researchers. Thereby, mechanical behaviors' studies are of a great interest for manufacture and engineering design (Zhang and Ou 2015, Liu *et al*. 2020, Yang *et al*. 2020, Zhang *et al*. 2020). One key issue in the mechanical engineering is energy management (Gao *et al*. 2016, Chen *et al*. 2017, He *et al*. 2018a, He *et al*. 2018b, Lu *et al*. 2019, Wang *et al*. 2019, Li *et al*. 2020, Lv *et al*. 2020, Shi *et al*. 2020, Shi *et al*. 2020, Wang *et al*. 2020, Yang *et al*. 2020, Zhang 2020, Zhao *et al*. 2020, Zhu *et al*. 2020, Zuo *et al*. 2020). For improving the energy management, and dynamics control performance, designers can use this kind of material for fabrication of the various applicable structures (Zhang and Ou 2008, Xu *et al*. 2014, Zhang 2014, Zhang and Wang 2019, Wang *et al*. 2020, Yu *et al*. 2020, Zhang and Wang 2020). Feng *et al* (Feng *et al*. 2017) suggested a new glass created using multi-layer composite polymer beams filled by GPLs for studying its nonlinear bending behavior. They proposed that symmetric distribution an increased GPLs' weight fraction in beams would lead to less sensitivity in the nonlinear deformation. Dong *et al*. 2020) studied nonlinear harmonic resonance behaviors of GPLRC spinning cylindrical thin shells subjected to a thermal load and an external excitation. One of their amazing results was that the Coriolis effect due to the spinning motion has a contribution to the damping terms of the system. Post-buckling and buckling characteristics of GPLs reinforcing composite dielectric beams were analyzed through mathematical formulation by Ref. (Wang *et al*. 2019). They demonstrated that the buckling of dielectric beams are highly sensitive to the AC current change within a specific range. Ref. (Dong *et al*. 2019) studied spinning cylindrical GPLRC shells' low-speed influence under impact, thermal and external axial loads through employing an exact study. Dong *et al*. (Dong *et al*. 2018) evaluated the cylindrical GPLRC shells' buckling with the motion of spinning and under an integrated action of external axial compressive force and radial pressure. They extracted the governing equations via von Kármán's geometrical nonlinearity and minimum potential energy principle. In their work, they specifically highlighted the influences of porosity factors, the cylindrical shells' scattering pattern, the weight fraction, the GPLs' configurational size, and rotational velocity on the wide range of structure's critical buckling load classes and structure's pre-buckling deformation. FG nanocomposite porous plates' free vibration and buckling boosted by GPLs using Chebyshev-Ritz approach was conducted by Ref. (Yang, Chen *et al*. 2018). They found that GPL nanofillers' geometric factors and weight fraction and the porosity factor have a vital contribution in the porous nanocomposite plates' vibration and buckling information. The theoretical along with experimental researches disclose that scale influences have significant contribution in their mechanical properties. However, inaccurate responses would be the result of eliminating the mentioned impacts. It, however, could be noted that, the size-dependency is not taken into account in the basic continuum models, then these models would not be able to be used in nano and micro sizes (Balubaid *et al*. 2019, Bedia *et al*. 2019, Berghouti *et al*. 2019, Boutaleb *et al*. 2019, Hussain *et al*. 2019, Karami *et al*. 2019, Semmah *et al*. 2019, Asghar *et al*. 2020, Bellal *et al*. 2020, Hussain *et al*. 2020, Matouk *et al*. 2020). However, there are approaches including simulation of molecular dynamic (MD), FE model along with non-classical continuum method which are likely to be used in analyzing nano-scaled structures. Simulations using MD contain time-consuming and complex computations which would be undesirable for researchers, while, efficient and simple, higher-order-continuum-mechanic models, have newly attracted scientists' attentions. As investigating the nano-scaled shells' mechanical performances pertains to dimensions of submicron, they would not be able to be predicted precisely by the basic model. Thereby, for size-dependency consideration, higher-order-continuum models are applied. These mentioned models contain the modified-couple-stress model, Eringen model, and nonlocal-strain-gradient method. Ref (Čanađija *et al*. 2016) has analyzed Bernoulli-Euler approach for modelling nano-sized beams employing fields of nonhomogeneous temperature, based on Eringen's approach. They, finally reported that reliable nonlocality and thermodynamically consistent would be applied to non-isothermal and non-homogenous situations. Employing a nonlocal thermodynamic model, Barreta *et al* reported a highly gradient elasticity for nanobeams' bending. The mentioned paper deals with an analytical approach for solving Clamped-Free nanobeam. In another work Barreta *et al*. 2018) scrutinized a stress-driven model to evaluate nanobeams' thermoelastic behavior applying the approach of nonlocal size-dependency.

In the field of static/dynamic analysis of the small-scaled structures of GPLRC, Sahmani *et al*. 2017) scrutinized GPLRC nano-sized shells' nonlinear instability subjected to hydrostatic pressure applying MSGT and nonlocality. Moreover (Sahmani and Aghdam 2017), they have analyzed GPLRC nano-sized shells' nonlinear instability under axials loads based on NSGT. It, however, could be mentioned that, MSGT is considered as a high-order-continuum model employing three types of length scale factors (Mirsalehi *et al*. 2017). The mentioned factors would by highly used in small-sized structures' simulation presented in the outcome step. However, in the structures' forced vibration area, Song *et al* (Song, Kitipornchai *et al*. 2017) studied FG composite polymer plates' forced and free vibration filled by GPLs. They investigated the impacts of GPL distribution types, configuration, weight function and overall layers' number, as well as, the size on the plates' dynamics. Atanasov *et al*. 2017), in another investigation have proposed orthotropic double-nanoplate system's Forced vibration employing nonlocal model. Their paper, applies an analytical approach to the orthotropic double-nanoplate systems' dynamics for a broad range of transversal external forces. Furthermore, Du *et al*. 2014) have analyzed FG cylindrical shells' nonlinear forced vibration which is infinitely long employing the multiple

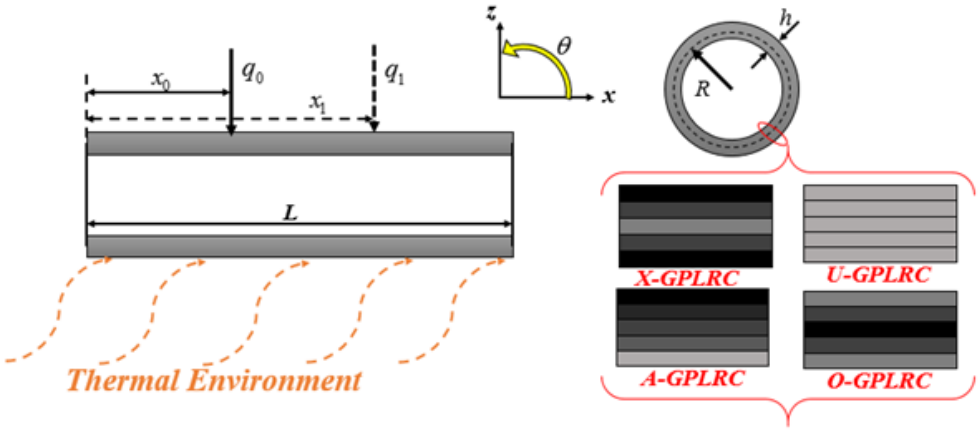

Fig. 1 Geometry of cylindrical FG nano-scaled shell subjected to dynamic load and thermal environment

scale approach and Lagrangian model. The most exciting outcome of their paper is that, power-law index have a vital contribution in the cylindrical FG shells' amplitude response. Li *et al*. 2018) scrutinized the axially and rotational moving thin-walled composite beam's dynamics. Their research dealt with a range of interesting results regarding the crucial rotational angular velocity and critical axial velocity. As another essential element in the composite nanostructures' design is an imperfection in the manufacturing processes appearing as porosity. Thereby, The mentioned imperfection should be taken into account in the modelling and simulation of nano-sized structures. For instance, an FG imperfect small-scaled plates' nonlinear large-amplitude dynamics filled by GPLs in the framework of NSGT has been scrutinized by Sahmani *et al*. 2018). Moreover, Barati *et al*. 2018 investigated heterogeneous nano-sized plates' forced vibration considering imperfections as porosity employing generalized NSGT. They disclosed that the nanoplate's forced vibration are highly affected by the frequency of excitation, nonlocality, porosities and location of dynamic load. Chen *et al*. (Chen *et al*. 2016) have studied slightly thick porous beam's nonlinear free vibration. Their paper used von Kármán class of nonlinear strain-displacement relations and Ritz approach for extracting the equations. Due to their results, ratio of slenderness, porosity factor, ratio of thickness and other factors have a prominent contribution in the slightly thick porous beam's nonlinear vibration. Moreover, Refs. (El-Hassar, Benyoucef *et al*. 2016; Fahsi, Tounsi *et al*. 2017; Issad *et al*. 2018, Sadoun *et al*. 2018, Younsi *et al*. 2018, Ahmed *et al*. 2019, Boulefrakh *et al*. 2019, Chikr *et al*. 2020, Rabhi *et al*. 2020) reported instability/stability structures' investigation using various solution processes.

For all we know, there are no investigations presented in the literature for analyzing thermal buckling employing changes of relative frequency. This study is a pioneering investigation in this field, revealing that thermal buckling would happen as long as if the percentage of the change of the relative frequency reaches to 30%. The newness of the present paper is applying distributions of multifarious temperature, GPLRC, size effects and dynamic load to the suggested model employing FMCS. Due to the high precision and analytical approaches' efficiency, it is applied to solve the problem's governing equations. The boundary conditions (BCs) and governing equations are extracted employing potential minimum energy which has been solved using an analytical approach. Eventually, using the previously-mentioned continuum mechanics model, the study is created considering the pattern of GPL distribution and thermal distribution impacts on the stability/instability, resonance frequency, relative frequency change and dynamic deflection of the system.

2. Mathematical model

The structure in the shape of cylindrical nano-sized shell in thermal situations and subjected to dynamic forces is mathematically modeled. The length, thickness, and the cylindrical shell's radius of middle surface are depicted by L, h, along with R, respectively. Moreover, transverse loads are denoted by q_0 according to inserted dynamic forces (Fig. 1).

Composite materials would create the modeled cylindrical nano-sized shell. There are four GPL distribution pattern types including U, X, O, A patterns in which volume fractions are as follows

$$\text{Pattern 1: } U-Pattern: \quad V_{GPL}(k)=V_{GPL}^{*} \tag{1}$$

Pattern 2:

$$X-Pattern: \quad V_{GPL}(k)=2V_{GPL}^{*}\left|2k-N_L-1\right|/N_L \tag{2}$$

Pattern 3:

$$O-Pattern: \quad V_{GPL}(k)=2V_{GPL}^{*}\left[1-\left(\left|2k-N_L-1\right|/N_L\right)\right] \tag{3}$$

Pattern 4:

$$A-Pattern: \quad V_{GPL}(k)=2V_{GPL}^{*}(2k-1)/N_L \tag{4}$$

here k is layers' number of the nano-sized shell, overall layers' number is denoted by N_L and V_{GPL}^{*} is the overall GPLs' volume fraction. The equation between their weight fraction $g_{GPL}$and V_{GPL}^{*} would be defined by

$$V_{GPL}^{*}=\frac{g_{GPL}}{g_{GPL}+(\rho_{GPL}/\rho_m)(1-g_{GPL})} \tag{5}$$

in which ρ_m and ρ_{GPL} are the polymer matrix's and GPLs' densities. Employing Halpin-Tsai approach, the following equations approximate composites' elastic modulus which is randomly reinforced by GPLs (Dong *et al*. 2018)

$$\begin{aligned} &E=\frac{3}{8}E_L+\frac{5}{8}E_T,\\ &E_L=\frac{1+\xi_L n_L V_{GPL}}{1-n_L V_{GPL}}E_m,\quad E_T=\frac{1+\xi_T n_T V_{GPL}}{1-n_T V_{GPL}}E_m \end{aligned} \tag{6}$$

here composites' effective Young modulus which is enhanced using GPLs is depicted by E. However, E_T and E_L are the transverse and longitudinal elasticity module for a lamina which is unidirectional. In Eq. (6) the GPL configuration factors ($\xi_L$and ξ_T) and other elements are presented by (Dong *et al*. 2018):

$$\begin{aligned} &\xi_L=2(\mathbb{Z}_{GPL}/h_{GPL}),\quad \xi_t=2(b_{GPL}/h_{GPL}),\\ &n_L=\frac{(E_{GPL}/E_m)-1}{(E_{GPL}/E_m)+\xi_L},\quad n_T=\frac{(E_{GPL}/E_m)-1}{(E_{GPL}/E_m)+\xi_T} \end{aligned} \tag{7}$$

here $\mathbb{Z}_{GPL}$,h_{GPL} ,b_{GPL} are the GPLs' thickness, width and mean length. By applying mixture rule, GPL/ polymer nanocomposite's mechanical properties are defined as

$$\begin{aligned} &\bar{E}=E_{GPL}V_{GPL}+E_M V_M,\\ &\bar{\rho}=\rho_{GPL}V_{GPL}+\rho_M V_M,\\ &\bar{\nu}=\nu_{GPL}V_{GPL}+\nu_M V_M,\\ &\bar{\alpha}=\alpha_{GPL}V_{GPL}+\alpha_M V_M. \end{aligned} \tag{8}$$

The cylindrical FG-GPLR shell's mechanical properties with a range of distribution classes would be achieved by (Sahmani, Aghdam *et al*. 2018):

Due to the FSDT, the cylindrical shell's displacement field through three directions of θ, x, z would be as follows

$$\begin{aligned} &u(z,\theta,x,t)=u_0(\theta,x,t)+z\psi_x(x,\theta,t)\\ &v(z,\theta,x,t)=v_0(\theta,x,t)+z\psi_\theta(x,\theta,t)\\ &w(z,\theta,x,t)=w_0(\theta,x,t) \end{aligned} \tag{9}$$

here, w_0 (x, θ, z), v_0 (x, θ, z) and u_0(x, θ, z) denotes the displacements in radial, circumferential and axial orientations, respectively. ψ_θ(x, θ,t) and ψ_x(x, θ, t) are the axial orientation and normal to the element middle plane's rotations about the circumferential. Moreover, the three-dimensional strain–stress equations may be defined as follows (Ghabussi *et al*. 2019, Habibi *et al*. 2019, Al-Furjan *et al*. 2020a, Al-Furjan *et al*. 2020b, Al-Furjan *et al*. 2020b, Al-Furjan *et al*. 2020c, Al-Furjan *et al*. 2020d, Al-Furjan *et al*. 2020e, Al-Furjan *et al*. 2020f Al-Furjan *et al*. 2020g, Al-*et al*. 2020h, Mohammadgholiha *et al*. 2020, Oyarhossein *et al*. 2020a, Oyarhossein *et al*. 2020b, Oyarhossein *et al*. 2020c, Safarpour *et al*. 2020a, Ebrahimi *et al*. 2020, Safarpour *et al*. 2020b, Moayedi *et al*. 2020a, Moayedi *et al*. 2020b, Oyarhossein *et al*. 2020c, Ghabussi *et al*. 2020, Shokrgozar *et al*. 2020):

$$\begin{bmatrix}\sigma_{xx}\\ \sigma_{\theta\theta}\\ \sigma_{zz}\\ \sigma_{x\theta}\\ \sigma_{xz}\\ \sigma_{\theta z}\end{bmatrix}=\begin{bmatrix}\bar{Q}_{11}&\bar{Q}_{12}&\bar{Q}_{13}&0&0&0\\ \bar{Q}_{12}&\bar{Q}_{22}&\bar{Q}_{23}&0&0&0\\ \bar{Q}_{13}&\bar{Q}_{23}&\bar{Q}_{33}&0&0&0\\ 0&0&0&\bar{Q}_{44}&0&0\\ 0&0&0&0&\bar{Q}_{55}&0\\ 0&0&0&0&0&\bar{Q}_{66}\end{bmatrix}\begin{bmatrix}\varepsilon_{xx}\\ \varepsilon_{\theta\theta}\\ \varepsilon_{zz}\\ \varepsilon_{x\theta}\\ \varepsilon_{xz}\\ \varepsilon_{\theta z}\end{bmatrix} \tag{10}$$

Ref (Barooti, Safarpour *et al*. 2017) would lead to obtaining Eq. (10) which defines the stiffness factors. Moreover, ΔT and α_i are (in x, θ along with z orientations) changes of temperature and thermal expansions, respectively. For the BCs' and motion's relations, the minimum energy approach states that:

$$\int_{t_1}^{t_2}(\delta T-\delta U+\delta W_1-\delta W_2)dt=0 \tag{11}$$

FMCS's Strain energy of cylindrical nano-sized shell is explained as

$$U=\frac{1}{2}\iiint_V(\sigma_{ij}\varepsilon_{ij}+m_{ij}^s\chi_{ij}^s)R\,dx d\theta dz \tag{12}$$

In Eq. (12) σ_{ij} and ε_{ij} denote the stress tensor and strain tensor elements explained in Ref (Barooti, Safarpour *et al*. 2017). Moreover, m_{ij} and χ_{ij}^s are the elements of a higher-order tensor of stress and spinning gradient symmetric tensor, which would be written as

$$\begin{aligned} &\chi_{ij}^s=\frac{1}{2}(\varphi_{i,j}+\varphi_{j,i})\\ &m_{ij}^s=2l^2\mu\chi_{ij}^s \end{aligned} \tag{13}$$

here l and φ_i respectively denote the MCS factor and highly small spinning vector, which is pertained to symmetric rotation gradients would be written as

$$l=l_{GPL}V_{GPL}+l_M V_M \tag{14}$$

However, the symmetric spinning gradient tensor's non-zero elements are achieved as

$$\begin{aligned} &\chi_{xx}^s=-\frac{1}{2}(\frac{\partial\psi_\theta}{\partial x}+\frac{1}{R}\frac{\partial v}{\partial x}-\frac{1}{R}\frac{\partial^2 w}{\partial x\partial\theta})\\ &\chi_{\theta\theta}^s=-\frac{1}{2R}(\frac{1}{R}\frac{\partial u}{\partial\theta}-\frac{\partial v}{\partial x}-z\frac{\partial\psi_\theta}{\partial x})-\frac{1}{2}(\frac{1}{R}\frac{\partial^2 w}{\partial x\partial\theta}-\frac{1}{R}\frac{\partial\psi_x}{\partial\theta})\\ &\chi_{zz}^s=-\frac{1}{2}(\frac{1}{R}\frac{\partial\psi_x}{\partial\theta}-\frac{\partial\psi_\theta}{\partial x}-\frac{1}{R^2}\frac{\partial u}{\partial\theta})\\ &\chi_{x\theta}^s=-\frac{1}{4}(\frac{1}{R^2}\frac{\partial v}{\partial\theta}+\frac{\partial^2 w}{\partial x^2}-\frac{1}{R^2}\frac{\partial^2 w}{\partial\theta^2}-\frac{\partial\psi_x}{\partial x}+\frac{1}{R}\frac{\partial\psi_\theta}{\partial\theta})\\ &\chi_{xz}^s=-\frac{1}{4}(\frac{1}{R}\frac{\partial^2 u}{\partial x\partial\theta}-\frac{\partial^2 v}{\partial x^2}-\frac{v}{R^2}+\frac{1}{R^2}\frac{\partial w}{\partial\theta}+\frac{\psi_\theta}{R})-\frac{z}{4}(\frac{1}{R}\frac{\partial^2\psi_\theta}{\partial x\partial\theta}-\frac{\partial^2\psi_\theta}{\partial x^2})\\ &\chi_{\theta z}^s=-\frac{1}{4}(\frac{1}{R^2}\frac{\partial^2 u}{\partial\theta^2}-\frac{1}{R}\frac{\partial^2 v}{\partial x\partial\theta}-\frac{1}{R}\frac{\partial w}{\partial x}+\frac{\psi_x}{R})-\frac{z}{4}(\frac{1}{R^2}\frac{\partial^2\psi_x}{\partial\theta^2}-\frac{1}{R}\frac{\partial^2\psi_\theta}{\partial x\partial\theta}) \end{aligned} \tag{15}$$

Ultimately, the non-classical and classical current study's strain energies based on FMCS elements are defined as

$$\frac{1}{2}\iiint_V(\sigma_{ij}\delta\varepsilon_{ij})dV=\iint_A\left\{\begin{array}{l}(N_{xx}\frac{\partial}{\partial x}\delta u+M_{xx}\frac{\partial}{\partial x}\delta\psi_x)+N_{\theta\theta}(\frac{1}{R}\frac{\partial}{\partial\theta}\delta v+\frac{\delta w}{R})+\\M_{\theta\theta}\frac{1}{R}\frac{\partial}{\partial\theta}\delta\psi_\theta+Q_{xz}(\delta\psi_x+\frac{\partial}{\partial x}\delta w)+\\N_{x\theta}(\frac{1}{R}\frac{\partial}{\partial\theta}\delta u+\frac{\partial}{\partial x}\delta v)+M_{x\theta}(\frac{1}{R}\frac{\partial}{\partial\theta}\delta\psi_x+\frac{\partial}{\partial x}\delta\psi_\theta)\\+Q_{z\theta}(\delta\psi_\theta+\frac{1}{R}\frac{\partial}{\partial\theta}\delta w-\frac{\delta v}{R})\end{array}\right\}Rdxd\theta$$

$$\frac{1}{2}\iiint_V(m_{ij}^s\delta\chi_{ij}^s)dV=\iint_A\left\{\begin{array}{l}(-\frac{Y_{\theta\theta}}{2R^2}+\frac{Y_{xz}}{2R^2})\frac{\partial}{\partial\theta}\delta u-(\frac{Y_{\theta z}}{2R^2})\frac{\partial^2}{\partial\theta^2}\delta u\\-(\frac{Y_{zx}}{2R})\frac{\partial^2}{\partial\theta\partial x}\delta u\\+(\frac{Y_{\theta\theta}}{2R}-\frac{Y_{xx}}{2R})\frac{\partial}{\partial x}\delta v+(\frac{Y_{xz}}{2})\frac{\partial^2}{\partial x^2}\delta v\\-(\frac{Y_{\theta x}}{2R^2})\frac{\partial}{\partial\theta}\delta v\\+(\frac{Y_{\theta z}}{2R})\frac{\partial^2}{\partial\theta\partial x}\delta v+(\frac{Y_{xz}}{2R^2})\delta v+(\frac{Y_{\theta z}}{2R})\frac{\partial}{\partial x}\delta w\\-(\frac{Y_{\theta x}}{2})\frac{\partial^2}{\partial x^2}\delta w\\-(\frac{Y_{zx}}{2R^2})\frac{\partial}{\partial\theta}\delta w+(\frac{Y_{x\theta}}{2R^2})\frac{\partial^2}{\partial\theta^2}\delta w+\\(-\frac{Y_{\theta\theta}}{2R}+\frac{Y_{xx}}{2R})\frac{\partial^2}{\partial\theta\partial x}\delta w\\+(\frac{Y_{x\theta}}{2})\frac{\partial}{\partial x}\delta\psi_x+(\frac{Y_{\theta\theta}}{2R}-\frac{Y_{xx}}{2R})\frac{\partial}{\partial\theta}\delta\psi_x\\-(\frac{T_{zx}}{2R})\frac{\partial^2}{\partial\theta\partial x}\delta\psi_x\\-(\frac{Y_{z\theta}}{2R})\delta\psi_x-(\frac{Y_{x\theta}}{2R})\frac{\partial}{\partial\theta}\delta\psi_\theta+\\(\frac{Y_{\theta\theta}}{2R}-\frac{Y_{xx}}{2}+\frac{Y_{zz}}{2})\frac{\partial}{\partial x}\delta\psi_\theta\\+(\frac{T_{z\theta}}{2R})\frac{\partial^2}{\partial\theta\partial x}\delta\psi_\theta-(\frac{T_{z\theta}}{2R^2})\frac{\partial^2}{\partial\theta^2}\delta\psi_x\\+(\frac{T_{xz}}{2})\frac{\partial^2}{\partial x^2}\delta\psi_\theta-(\frac{Y_{xz}}{2R})\delta\psi_\theta\end{array}\right\}Rdxd\theta \quad (16)$$

where parameters used in above equation are explained as

$$\begin{aligned}&(N_{xx},N_{\theta\theta},N_{x\theta})=\int_{-h/2}^{h/2}(\sigma_{xx},\sigma_{\theta\theta},\sigma_{x\theta})dz,\\&(M_{xx},M_{\theta\theta},M_{x\theta})=\int_{-h/2}^{h/2}(\sigma_{xx},\sigma_{\theta\theta},\sigma_{x\theta})zdz,\\&(Q_{xz},Q_{z\theta})=\int_{-h/2}^{h/2}k_s(\sigma_{xz},\sigma_{z\theta})dz,\\&(Y_{xx},Y_{\theta\theta},Y_{zz},Y_{x\theta},Y_{xz},Y_{z\theta})=\int_{-h/2}^{h/2}(m_{xx},m_{\theta\theta},m_{zz},m_{x\theta},m_{xz},m_{z\theta})dz,\\&(T_{xx},T_{\theta\theta},T_{zz},T_{x\theta},T_{xz},T_{z\theta})=\int_{-h/2}^{h/2}(m_{xx},m_{\theta\theta},m_{zz},m_{x\theta},m_{xz},m_{z\theta})zdz\end{aligned} \quad (17)$$

Furthermore, the FG-GRCs cylindrical nano-scaled shell's kinetic energy using MCS element would be expressed as

$$\delta T=\int_Z\iint_A\rho\left\{\begin{array}{l}(\frac{\partial u}{\partial t}+z\frac{\partial\psi_x}{\partial t})(\frac{\partial}{\partial t}\delta u+z\frac{\partial}{\partial t}\delta\psi_x)\\+(\frac{\partial v}{\partial t}+z\frac{\partial\psi_\theta}{\partial t})(\frac{\partial}{\partial t}\delta v+z\frac{\partial}{\partial t}\delta\psi_\theta)+(\frac{\partial w}{\partial t})\frac{\partial}{\partial t}\delta w\end{array}\right\}R\,dz\,dx\,d\theta \quad (18)$$

In the current study, it is suggested that the temperature may be distributed through-thickness direction as presented by Refs. (Abualnour *et al*. 2019, Belbachir *et al*. 2019, Hellal *et al*. 2019, Mahmoudi *et al*. 2019, Zarga *et al*. 2019, Boussoula *et al*. 2020, Matouk *et al*. 2020, Refrafi *et al*. 2020, Tounsi *et al*. 2020). So, the work conducted in the result of temperature change would be explained as

$$W_1=\frac{1}{2}\iint_A\left[N_1^T(\frac{\partial w_0}{\partial x})^2+N_2^T(\frac{\partial v_0}{\partial x})^2\right]R\,dx\,d\theta \quad (19)$$

here N_2^T and N_1^T are the thermal resultants. It is worth to mention that the two thermal outcomes would be obtained as

$$\begin{aligned}N_1^T&=\int_{-h/2}^{h/2}(\bar{Q}_{11}+\bar{Q}_{12}+\bar{Q}_{13})\,\alpha(T-T_0)dz,\\N_2^T&=\int_{-h/2}^{h/2}(\bar{Q}_{21}+\bar{Q}_{22}+\bar{Q}_{23})\,\alpha(T-T_0)dz.\end{aligned} \quad (20)$$

Also, thermal expansion factors are

$$\alpha=\begin{bmatrix}\alpha_{xxe} & \alpha_{\theta\theta e} & \alpha_{zze} & 0 & 0 & 0\end{bmatrix}^T \quad (21)$$

2.1. Linear temperature changes

In the linear form of the temperature distribution, the temperature shifts would be explained as (Shahsiah and Eslami 2003)

$$T=T_c-\Delta T(\frac{1}{2}+\frac{z_c}{h}) \quad (22a)$$

2.2. Nonlinear temperature changes

In this case, nonlinear temperature changes may be defined as (Shafiei, Mirjavadi *et al*. 2017).

$$T=T_c-\Delta T(\frac{1}{2}+\frac{z_c}{h})^{\alpha_p} \quad (22b)$$

in which α_p presents the index of variation function of temperature power, for instance, using $\alpha_p \geq 2$ the variation of temperature through thickness will be nonlinear. The work conducted by inserted forces will be explained as

$$W_2=\frac{1}{2}\left\{q_{dynamic}w^2\right\}R\,dV \quad (23)$$

Transverse force is likely to be denoted by q $_{\text{dynamic}}$ representing inserted dynamic load. However, by inserting Eqs. (12), (18), (19) and (23) into Eq. (11) and by part integration, the GPL cylindrical nano-scaled shell's BCs and motion equations in thermal situations employing MCS factor would be achieved as:

$$\begin{aligned}&\left[\frac{\partial N_{xx}}{\partial x}+\frac{1}{R}\frac{\partial N_{x\theta}}{\partial\theta}+\frac{1}{2R^2}(-\frac{\partial Y_{\theta\theta}}{\partial\theta}+\frac{\partial Y_{zz}}{\partial\theta})+\frac{1}{2R}\frac{\partial^2 Y_{zx}}{\partial\theta\partial x}+\frac{1}{2R^2}\frac{\partial^2 Y_{\theta z}}{\partial\theta^2}\right]\delta u\\&+\left[\frac{\partial N_{x\theta}}{\partial x}+\frac{1}{R}\frac{\partial}{\partial\theta}N_{\theta\theta}+\frac{Q_{z\theta}}{R}+\frac{1}{2}\left\{\begin{array}{l}\frac{1}{R}\frac{\partial}{\partial x}(-Y_{xx}+Y_{\theta\theta})\\-\frac{1}{R^2}\frac{\partial Y_{\theta x}}{\partial\theta}-\frac{\partial^2 Y_{xz}}{\partial x^2}-\frac{Y_{xz}}{R^2}-\frac{1}{R}\frac{\partial^2 Y_{z\theta}}{\partial\theta\partial x}\end{array}\right\}\right]\delta v\\&-N_2^T\frac{\partial^2 v}{\partial x^2}\delta v+\left[\begin{array}{l}\frac{\partial Q_{xz}}{\partial x}+\frac{1}{R}\frac{\partial Q_{z\theta}}{\partial\theta}-\frac{N_{\theta\theta}}{R}-\frac{1}{2R^2}\frac{\partial^2 Y_{\theta x}}{\partial\theta^2}\\-\frac{1}{2R^2}\frac{\partial Y_{zx}}{\partial\theta}+\frac{1}{2R}\frac{\partial Y_{\theta z}}{\partial x}+\frac{\partial^2 Y_{x\theta}}{2\partial x^2}\end{array}\right]\delta w_0\\&+\left[-\frac{1}{2R}\frac{\partial^2}{\partial\theta\partial x}(Y_{xx}-Y_{\theta\theta})-N_1^T\frac{\partial^2 w}{\partial x^2}\right]\delta w_0+\left[\begin{array}{l}\frac{\partial M_{xx}}{\partial x}+\frac{1}{R}\frac{\partial M_{\theta\theta}}{\partial\theta}-Q_{xz}\\+\frac{1}{2}\frac{\partial Y_{\theta x}}{\partial x}-\frac{1}{2R}\frac{\partial}{\partial\theta}(Y_{zz}-Y_{\theta\theta})\end{array}\right]\delta\psi_x\\&+\left[\frac{Y_{zz}}{R}+\frac{1}{2R}\frac{\partial^2 T_{zx}}{\partial\theta\partial x}+\frac{1}{2R^2}\frac{\partial^2 T_{\theta z}}{\partial\theta^2}\right]\delta\psi_x+\left[\begin{array}{l}\frac{1}{R}\frac{\partial M_{\theta\theta}}{\partial\theta}+\frac{\partial M_{x\theta}}{\partial x}-Q_{z\theta}\\+\frac{1}{2}\frac{\partial}{\partial x}(Y_{zz}-Y_{xx}+\frac{T_{\theta\theta}}{R})\end{array}\right]\delta\psi_\theta\\&+\left[-\frac{1}{2}\frac{\partial Y_{\theta x}}{\partial\theta}+\frac{Y_{xz}}{2R}-\frac{1}{2R}\frac{\partial^2 T_{\theta z}}{\partial\theta\partial x}-\frac{1}{2}\frac{\partial^2 T_{zx}}{\partial x^2}\right]\delta\psi_\theta=\left\{I_0\frac{\partial^2 u}{\partial t^2}+I_1\frac{\partial^2\psi_x}{\partial t^2}\right\}\delta u\\&+\left\{I_0\frac{\partial^2 v}{\partial t^2}+I_1\frac{\partial^2\psi_\theta}{\partial t^2}\right\}\delta v+I_0\frac{\partial^2 w}{\partial t^2}\delta w_0+\left\{I_1\frac{\partial^2 u}{\partial t^2}+I_2\frac{\partial^2\psi_x}{\partial t^2}\right\}\delta\psi_x\\&+\left\{I_1\frac{\partial^2 v}{\partial t^2}+I_2\frac{\partial^2\psi_\theta}{\partial t^2}\right\}\delta\psi_\theta+q_{dynamic}\delta w\end{aligned} \quad (24)$$

Table1 Comparison of non-dimensional first three natural frequencies of isotropic homogeneous nano-scaled shells, with a range of thicknesses, m=1 and L/R=10.

h/R	n	Ref (Tadi Beni, Mehralian *et al*. 2016) (l=0)	Present (l=0)	Ref (Tadi Beni, Mehralian *et al*. 2016) (l=h)	Present study (l=h)
0.02	1	0.1954	0.19536215	0.1955	0.19543206
	2	0.2532	0.25271274	0.2575	0.25731258
	3	0.2772	0.27580092	0.3067	0.30621690
0.05	1	0.1959	0.19542305	0.1963	0.19585782
	2	0.2623	0.25884786	0.2869	0.28543902
	3	0.3220	0.31407326	0.4586	0.45457555

In addition, governing equations and BCs are given in the appendix.

3. Solution procedure

The current step proposes an analytical approach for solving the complicated governing equations of MSGT-based on GPLRC small-sized shell. However, this research dealt with modeling a simply-supported shell in which x=L, 0 and θ=$\pi/2,3\pi/2$. Then, the field of displacements are likely to be computed as:

$$\begin{Bmatrix} u_0(x,\theta,t) \\ v_0(x,\theta,t) \\ w_0(x,\theta,t) \\ \psi_x(x,\theta,t) \\ \psi_\theta(x,\theta,t) \end{Bmatrix} = \sum_{m=1}^{\infty}\sum_{n=1}^{\infty} \begin{Bmatrix} U_{0mn}\cos(\frac{m\pi}{L}x)\cos(n\theta) \\ V_{0mn}\sin(\frac{m\pi}{L}x)\sin(n\theta) \\ W_{0mn}\sin(\frac{m\pi}{L}x)\cos(n\theta) \\ \Psi_{xmn}\cos(\frac{m\pi}{L}x)\cos(n\theta) \\ \Psi_{\theta mn}\sin(\frac{m\pi}{L}x)\sin(n\theta) \end{Bmatrix} \sin(\omega t) \quad (25)$$

here $\{U_{0mn}, V_{omn}, W_{0mn}, \Psi_{xmn}, \Psi_{\theta mn}\}$ would be the unknown Fourier factors that need to be achieved for all m and n amounts. Moreover, m and n could be defined as numbers of the axial wave and circumferential, respectively. For structure's vibration investigation, by inserting Eq. (25) into governing relations, one achieves

$$\left(\begin{Bmatrix} K_{11} & K_{12} & K_{13} & K_{14} & K_{15} \\ K_{21} & K_{22} & K_{23} & K_{24} & K_{25} \\ K_{31} & K_{32} & K_{33} & K_{34} & K_{35} \\ K_{41} & K_{42} & K_{43} & K_{44} & K_{45} \\ K_{51} & K_{52} & K_{53} & K_{54} & K_{55} \end{Bmatrix} - \omega^2 \begin{Bmatrix} M_{11} & M_{12} & M_{13} & M_{14} & M_{15} \\ M_{21} & M_{22} & M_{23} & M_{24} & M_{25} \\ M_{31} & M_{32} & M_{33} & M_{34} & M_{35} \\ M_{41} & M_{42} & M_{43} & M_{44} & M_{45} \\ M_{51} & M_{52} & M_{53} & M_{54} & M_{55} \end{Bmatrix} \right) \begin{Bmatrix} U_0 \\ V_0 \\ W_0 \\ \psi_x \\ \psi_\theta \end{Bmatrix} = \begin{bmatrix} 0 \\ 0 \\ q_{dynamic} \\ 0 \\ 0 \end{bmatrix} \begin{Bmatrix} U_0 \\ V_0 \\ W_0 \\ \psi_x \\ \psi_\theta \end{Bmatrix} \quad (26)$$

It may be essential to mention that mass elements and stiffness are presented in the paper's appendix. In Eq. (26), natural frequency is shown by ω and inserted dynamic load ($q_{dynamic}$) is written as

$$q_{dynamic} = \sum_{m=1}^{\infty}\sum_{n=1}^{\infty} q_0 \sin(\frac{m\pi}{L}x)\cos(n\theta)\sin(\omega t), \quad (27)$$

Table 2 Comparisons of natural frequencies parameters ($\omega/2\pi$) of simply-supported isotropic cylindrical shell with L=0.2 m, r=0.1 m, and h=0.247×10^{-3} m

n	Ref. (Dong, Zhu *et al*. 2018)	Ref. (Pellicano 2007)	Presented study
7	488.424	484.6	487.598563
8	494.495	489.6	493.659826
9	551.750	546.2	550.598563
10	642.650	636.8	641.985639

Table 3 Epoxy's and GPL's Material properties (Wu, Kitipornchai *et al*. 2017)

Material properties	Epoxy	GPL
Young's modulus (GPa)	3	1010
Density (kg m^{-3})	1200	1062.5
Poisson's ratio	0.34	0.186
Thermal expansion coefficient(10^{-6}/K)	60	5

Eq. (27)'s Solution provides the imperfect FG-GPLRC cylindrical small-scaled shell's deflection related to dynamics and its excitation frequency. The forced vibration amplitude and nondimensional excitation frequency are explained as

$$\Omega = 10\times\omega L\sqrt{\rho/E}, \qquad \bar{W}_{uniform} = W_{0mn}\frac{10Eh^3}{L^4 q_0} \quad (28)$$

For finding the system's natural frequency and crucial temperature, by setting the factor matrix of the Eq. (26)'s determinant, an analytical approach may be achieved by the next relations

$$\left(\left[K_{ij}\right] + \Delta T\left[K_T\right] - \omega^2\left[M\right] \right) \begin{Bmatrix} U_0 \\ V_0 \\ W_0 \\ \psi_x \\ \psi_\theta \end{Bmatrix} = 0 \quad (29)$$

Where[K_T] and [K_{ij}] are temperature shift's coefficient matrix and stiffness matrix, respectively, and M denotes the matrix of mass. However, By equaling this polynomial to 0,

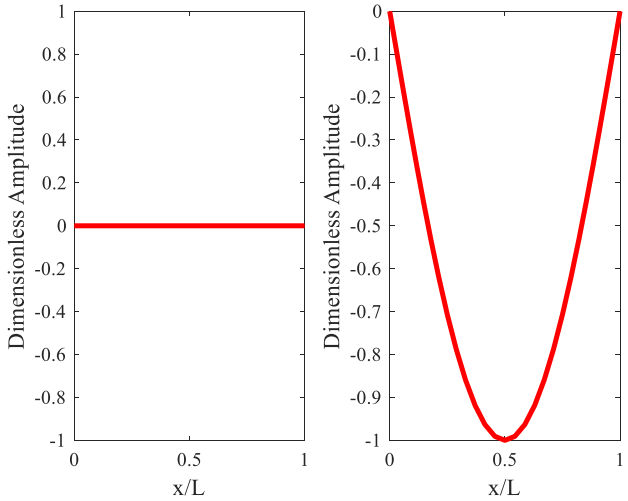

Fig. 2 The cylindrical nanoshell's mode shapes of thermal buckling in this research

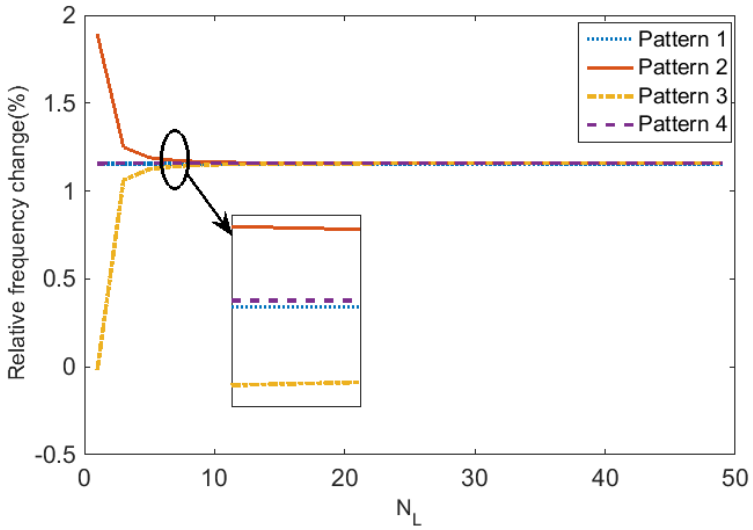

Fig. 3 Overall number of layers' influence of *NL* on the proportion of first frequency shift for multifarious GPL/epoxy's patterns ($\Delta T = 10K$, *l*=R/3, Pattern2, L/R=10, R/h=10 and n=m=1)

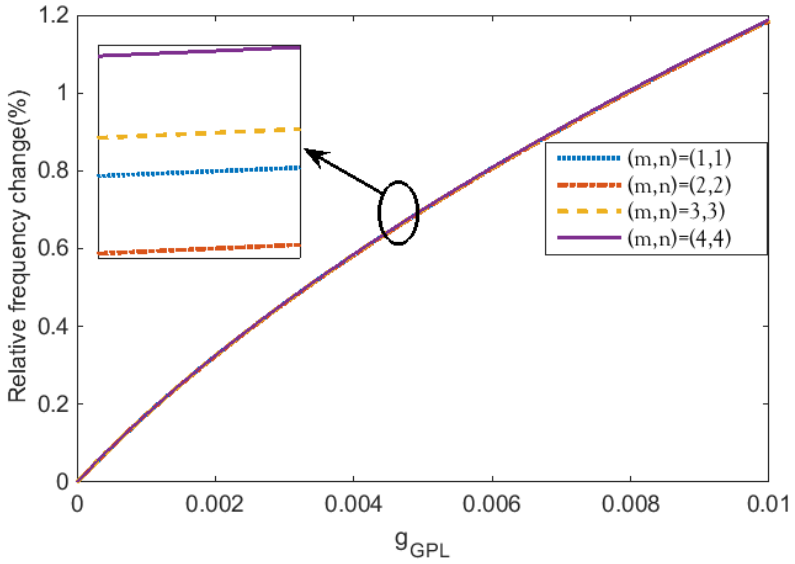

Fig. 4 Weight function's impact on the percentage of first natural frequency shift for various mode numbers ($\Delta T = 10K$, *l*=R/3, Pattern2, L/R=10, R/h=10)

we would be likely to obtain the system's natural frequencies (ω).

4. Validation

A comparison investigation has been conducted by Table 1 demonstrating this paper's outcomes and those published by considering simply-supported nano-sized shell using a model of modified-couple-stress. It would be observed that our achieved results are in keeping with the outcomes of Ref (Tadi Beni *et al*. 2016a). Moreover, in Ref. (Tadi Beni *et al*. 2016b), the impacts of thermal environment, GPL, and inserted load are neglected. The outcomes are revealed in Table 1 and the material properties considered in this study are as E=1.06 TPa, R=2.32 nm, ν=0.3 and L/R=5.

To conduct more validation for this research, it could be shown that the reported modeling would create results which are in line with Refs, due to Table 2, (Pellicano 2007, Dong *et al*. 2018), where the effects of length scale elements, thermal forces, and nonlinearity are eliminated. The shell's kinematics is established according to classical in Ref. (Dong *et al*. 2018), while in this study, the governing equations are defined according to FSDT. The material properties used in this comparison are considered as E= 71.02 GPa, ν =0.31, and $\rho = 2796kg/m^3$.

5. Results and discussion

The current step is supposed to disclose analytical outcomes for the BC of SS of a GPL cylindrical nano-sized shell located in a thermal situation subjected to a range of thermal forces. In the current research, the nano-sized structure GPL considering length of a_{GPL}=2.5μm, overall thickness of h_{GPL}=1.5 nm, and R_{GPL} =0.75μm which is the structure's radius. Table 3 is containing GPL's mechanical properties. Then, in this section the impacts of the various factors on the structure's dimensionless amplitude, excitation frequency and relative frequency shifts have been reported in detail.

Temperature dependent of the GPL materials is shown as follow (Wu *et al*. 2017):

E=(3.52- 0.0034T) GPa, and α_m=45(1+0.0005ΔT)x$10^{-6}/K$ in which T=T_0+ΔT.

Fig. 2 reveals cylindrical small-scaled shell's thermal buckling mode shape respected to the non-dimensional length of cylindrical shell. For having a much better mode shapes' insight, the nano-sized shell's vertical displacement is non-dimensioned due to the thermal buckling mode shape's maximum displacement.

The amount demonstrated in parentheses in percentage scale depicts the increasing the relative frequenc (ω_c- ω_M) in which ω_M and ω_c respectively, are considered as natural frequencies without and with GPL. Figure 3 reveals the FG-GPLRC cylindrical nano-sized shell's relative frequency shifts considering multifarious overall layers' number (N_L). As it was expected, the structure's fundamental frequencies using pattern of GPLs' distribution are under effects of N_L due to their homogeneous property. First natural frequency drops as overall layers' number reach to N_L=7, according to pattern 2 distribution type. Afterward, while N_L is soared up, they remain almost steady. However, pattern 3in GPL distribution experiences exactly a reverse trend. Amongst the three types of non-uniform considered patterns, the first mode of structure's natural frequency considering patterns 1 in GPL distribution. and pattern 4 would be least influenced by the shift in N_L. Due to this figure by increasing the layers' number ($1<N_L<7$) the nanostructure's stability and natural frequency alter (for patterns 3 and 2 in GPL distribution which are non-uniform). It would be seen that, pattern 3 in GPL distribution which is a non-uniform pattern, by raising the layers' number, the nanostructure's stability and natural frequency increase. However, for the other non-uniform and uniform patterns of distribution, GPL's number of layers would be not essential. Another significant outcome would be that, by soaring up the layers' number in pattern 2, the stability and natural frequency drop.

Fig. 4 discloses the impacts of weight function and mode number on the cylindrical GPL nano-sized shell's relative frequency shift. Considering Fig. 4, a mode number's increase would lead to a boost in the relative frequency, while it decreases the structure's stability. A considerable outcome would be that; weight function contributes directly in the GPL cylindrical nano-sized shell's shift of relative frequency. This phenomenon is happened based on softening the structure by raising the weight function. It would be a reason for soaring up the relative frequency shift.

A range of GPL pattern of distributions is affected due to the Table 4. The mentioned table shows the impacts of thermal distribution and FMCS factor on GPL's natural frequency of the nano-scaled structure. It would be observable that by raising pattern of GPL distribution by 3 from 1 to 4, the natural frequency behavior depends on the pattern's classes. For instance, the GPL's patterns 3 and 2 show the lower and higher natural frequency. As another example, more stability belongs to pattern 2 of GPL distribution in contrast with other types of patterns. It would be realized that the natural frequency would increase by raising the FMCS factor to radius ratio (l/R). However, the outcomes disclose that the nonlinear temperature shift (NLT) contributes much more considerable in natural frequency compared with the linear temperature shift (LT).

MCS's and classic theories' influences the GPL's relative frequency shifts of the cylindrical nano-scaled shell, respectively, have been illustrated by figure 5 and figure 6. Based on the mentioned figures, whenever the temperature change is increased, the relative frequency would be boosted and the structure's stability would be decreased. In other words, the relative frequency will be increased slightly by increasing temperature change. At a specific amount of temperature change, a considerable increase in structure's relative frequency would be seen. The occurred phenomena is due to the buckling behavior at this temperature. The significant outcome is that, MCS model

Table 4 The impacts of various FMCS factors to radius ratio, pattern of GPL and temperature on natural frequency (GHz) of the GPLRC nano-sized shell with L/R=10, R/h=10, g_{GPL}=1% and a range of distributions of temperature changes

		ΔT =20		ΔT =40		ΔT =60	
		LT	NLT	LT	NLT	LT	NLT
	l/R						
	0	1.948752	1.982586	1.904938	1.973578	1.859902	1.964363
Pattern 1	1/3	2.070645	2.102498	2.028391	2.092946	1.985038	2.083173
	1/2	2.184729	2.214933	2.143707	2.204870	2.101676	2.194574
	2/3	2.302991	2.331662	2.263052	2.321068	2.222178	2.310231
	l/R						
	0	1.947517	1.981282	1.903786	1.972283	1.858836	1.963078
Pattern 2	1/3	2.069517	2.101302	2.027344	2.091759	1.984077	2.081997
	½	2.183646	2.213784	2.142704	2.203735	2.100757	2.193447
	2/3	2.301909	2.330516	2.262047	2.319933	2.221255	2.309107
	l/R						
	0	1.951057	1.984761	1.907392	1.975764	1.862513	1.966560
Pattern 3	1/3	2.072872	2.104606	2.030755	2.095065	1.987547	2.085304
	1/2	1.186938	2.217031	2.146045	2.206980	2.104149	2.196697
	2/3	2.305233	2.333800	2.265415	2.323218	2.224670	2.312393
	l/R						
	0	1.949577	1.983336	1.905848	1.974335	1.860901	1.965126
Pattern 4	1/3	2.073030	2.104788	2.030885	2.095243	1.987647	2.085479
	1/2	2.188392	2.218488	2.147493	2.208434	2.105592	2.198148
	2/3	2.307948	2.336501	2.268143	2.325918	2.227411	2.315091

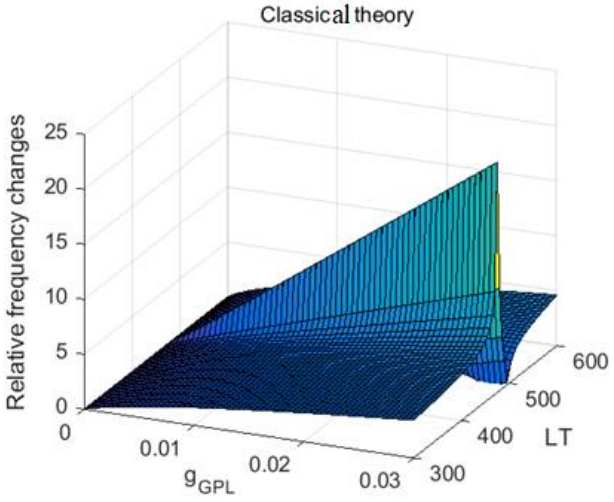

Fig. 5 The influences of temperature change and classical model on the relative frequency change for linear temperature change (LT) and various weight function (Pattern4, R/h=10 n=m=1and L/R=10)

has more influence on the structure's critical temperature compared with the classic model. Thereby, for simulating the small-sized structures, it would be attended to the theories of size dependency specially MCS model. Moreover, weight function contributes directly in the GPL cylindrical small-scaled shell's relative frequency shifts. This is due to the fact that, by raising the weight function, the structure would be softer and it is a basis of raising the relative frequency shift.

In Fig. 7 the weight function's impact on resonance frequency and dynamic deflection has been reported for the GPL nano-sized structure. However, in this figure, various amounts function (g_{GPL}) impact have been evaluated. It is proved that, cylindrical GPL nano-sized shell's dynamic deflection has been affiliated by the amount of dynamic load's excitation frequency. In other words, by raising the excitation frequency, it would be seen a slight increase in dynamic deflection. At an excitation frequency's certain amount, a considerable increase in cylindrical GPL nano-sized shell's deflection has been observed. It would be due to the fact that the resonance would happen, as long as the dynamic deflection would be infinity. By dropping the weight function, it could be seen that, GPL cylindrical nano-sized shell's resonance would drop as well. It would also be due to the fact that, structure's resonance frequency, stiffness and stability would boost due to raising weight

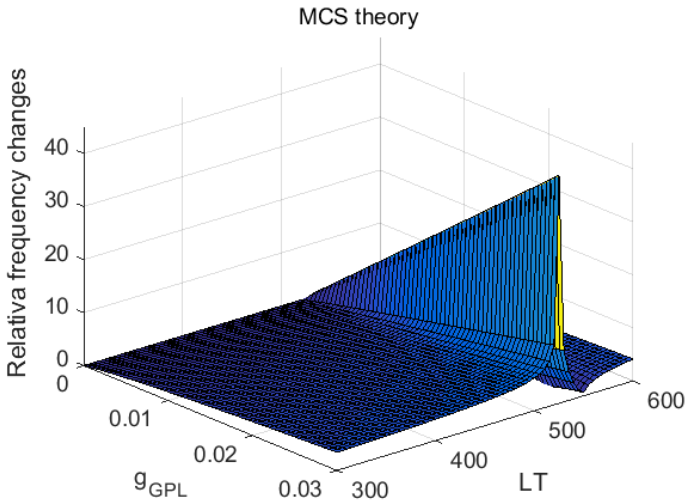

Fig. 6 The effects of temperature change and MCS model on the relative frequency change for a linear temperature change (LT) and range of weight functions (Pattern4, , R/h=10 n=m=1and L/R=10)

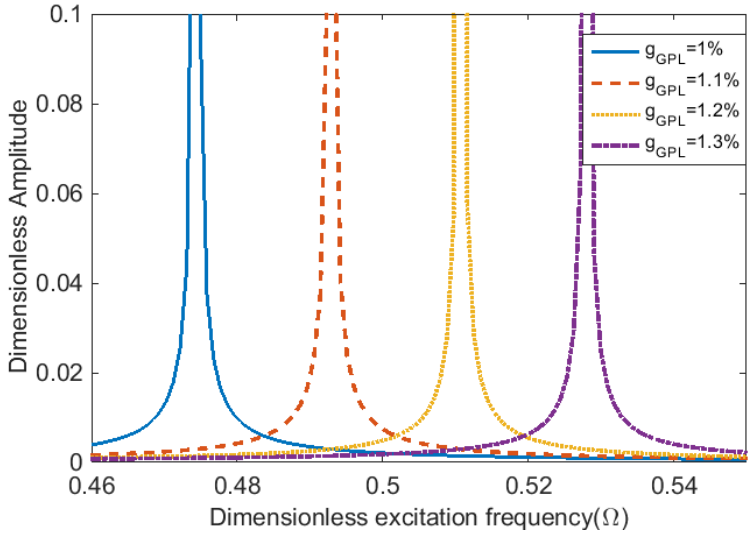

Fig. 7 Cylindrical nano-scaled shell's resonance frequency and dynamic deflection of the for various weight function ($\Delta T = 20K$, *l*=R/3, Pattern2, R/h=10 n=m=1 and L/R=10)

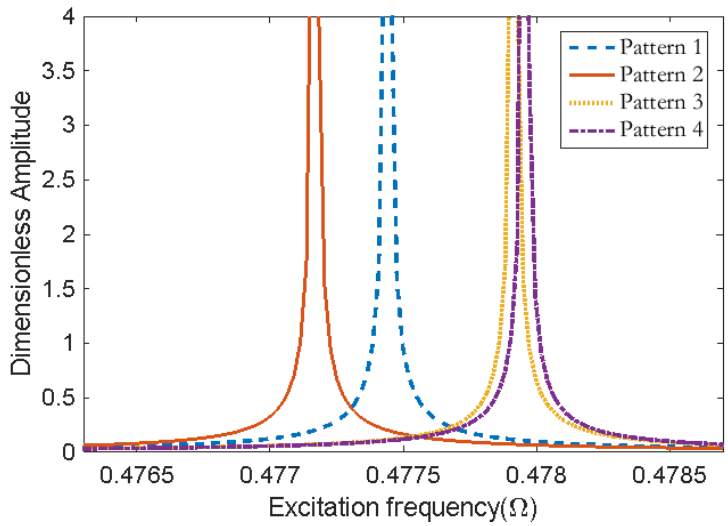

Fig. 8 The cylindrical nano-sized shell's resonance frequency and dynamic deflection for various patterns of GPL distribution ($\Delta T = 20K$, *l*=R/3, R/h=10 n=m=1and L/R=10)

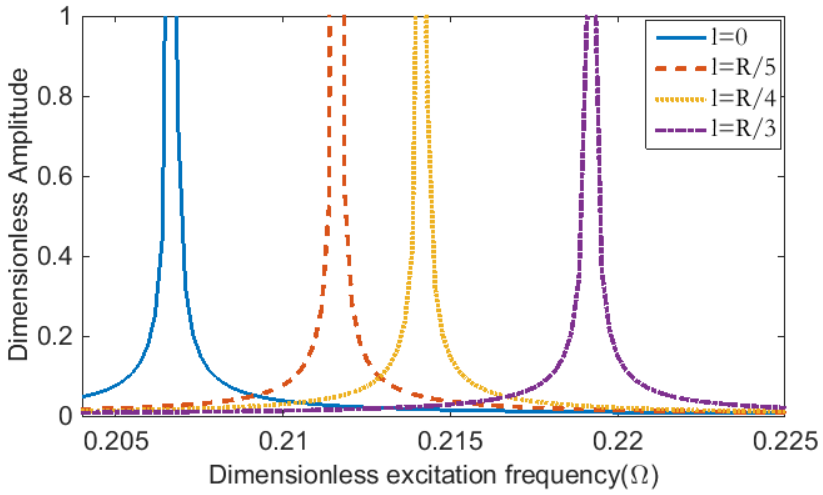

Fig. 9 cylindrical nano-sized shell's resonance frequency and dynamic deflection for various modified-couple-stress factor ($\Delta T = 20K$,Pattern2, R/h=10 n=m=1and L/R=10)

function.

In Fig. 8 the influence of a range of patterns of GPL distribution on GPL small-scaled structure's resonance frequency and dynamic deflection is revealed. It could be observed from the mentioned figure that as the pattern of GPL distribution increases by 3 from 1 to 4, the resonance frequency increases, it leads to a drop in the structure's instability. It means A-GPLRC provides higher resonance frequency rather than others. Moreover, the structure's resonance frequency, in the 4th pattern is much more similar to the 3rd pattern. The could be due to the fact that, this issue is in the mathematical function which is reported in last section.

In Fig. 9, the influences of FMCS factor on GPL cylindrical nano-sized shell's forced vibration for the pattern of X-GPLRC is reported. As a prominent outcome would observe that the FMCS element dramatically affects on the structure's resonance frequency. It will be understood from the figure, by boosting the FMCS element, the structure's resonance frequency would increases. However, this phenomenon enhances the GPL cylindrical nano-scaled shell's stability. It, however, could be noted that, as the FMCS factor is zero, the classic model occurs.

6. Conclusions

This research paper provides an investigation into the composite cylindrical shell's size-dependent forced and free vibration behaviors filled by GPL subjected to a range of thermal distributions in thermal situations. The GPL size-dependent shell is investigated considering FMCS factor. The non-classic BCs and relation of motion are extracted considering the minimum energy principle. Moreover, the current model's results have been verified using those achieved by simulation of molecular dynamics (MD). The impact of some vital factors including a range of thermal forces, patterns of GPL distribution, length to radius ratio, modified-couple-stress factor, thermal environment and mode number on the relative frequency shift, resonance frequency and GPL's dynamic deflection has been analyzed. In this scrutinization, the following key outcomes would be obtained:

- nonlinear change of temperature has much more contribution in the natural frequency comparing with the linear changes of temperature, according to the illustrated results.
- It is proved that an increase in resonance frequency is when weight function and the modified-couple-stress factor increase, and a drop would occur when the temperature nuances increase.
- Due to the reported results, A-GPL provides a higher resonance frequency comparing with others.
- An increase in the change of temperature would lead to an increase in the change of relative frequency and a drop in the structure's stability, according to the provided results
- By increasing the ratio of radius-to-thickness, the cylindrical GPL nano-scaled shell's stability and resonance frequency would increase.

Acknowledgements

This work was supported by Foundation Enhancement Programme Fund (2019-JCJQ-JJ-012).

References

Abualnour, M., Chikh, A., Hebali, H., Kaci, A., Tounsi, A., Bousahla, A.A. and Tounsi, A. (2019), "Thermomechanical analysis of antisymmetric laminated reinforced composite plates using a new four variable trigonometric refined plate theory", *Comput. Concrete*. **24**(6), 489-498. https://doi.org/10.12989/cac.2019.24.6.489

Ahmed, R.A., Fenjan, R.M. and Faleh, N.M. (2019), "Analyzing post-buckling behavior of continuously graded FG nanobeams with geometrical imperfections", *Geomech. Eng.*, **17**(2), 175-

180. https://doi.org/10.12989/gae.2019.17.2.175.
Al-Furjan, M., Alzahrani, B., Shan, L., Habibi, M. and Jung, D.W. (2020), "Nonlinear forced vibrations of nanocomposite-reinforced viscoelastic thick annular system under hygrothermal environment", *Mech. Based Des. Struct. Machines*. 1-27. https://doi.org/10.1080/15397734.2020.1824795.
Al-Furjan, M., Bolandi, S.Y., Shan, L., Habibi, M. and Jung, D.W. (2020), "On the vibrations of a high-speed rotating multi-hybrid nanocomposite reinforced cantilevered microdisk", *Mech. Based Des. Struct. Machines*. 1-29. https://doi.org/10.1080/15397734.2020.1828098.
Al-Furjan, M., Fereidouni, M., Habibi, M., Abd Ali, R., Ni, J. and Safarpour, M. (2020), "Influence of in-plane loading on the vibrations of the fully symmetric mechanical systems via dynamic simulation and generalized differential quadrature framework", *Eng. Comput*., 1-23. https://doi.org/10.1007/s00366-020-01177-7.
Al-Furjan, M., Habibi, M. and Safarpour, H. (2020), "Vibration control of a smart shell reinforced by graphene nanoplatelets", *Int. J. Appl. Mech*., https://doi.org/10.1142/S1758825120500660.
Al-Furjan, M., Habibi, M., Chen, G., Safarpour, H., Safarpour, M. and Tounsi, A. (2020), "Chaotic oscillation of a multi-scale hybrid nano-composites reinforced disk under harmonic excitation via GDQM", *Compos. Struct*., 112737. https://doi.org/10.1016/j.compstruct.2020.112737.
Al-Furjan, M., Habibi, M., Chen, G., Safarpour, H., Safarpour, M. and Tounsi, A. (2020), "Chaotic oscillation of a multi-scale hybrid nano-composites reinforced disk under harmonic excitation via GDQM", *Compos. Struct*., **252** 112737. https://doi.org/10.1016/j.compstruct.2020.112737.
Al-Furjan, M., Habibi, M., Chen, G., Safarpour, H., Safarpour, M. and Tounsi, A. (2020), "Chaotic simulation of the multi-phase reinforced thermo-elastic disk using GDQM", *Eng. Comput*., 1-24. https://doi.org/10.1007/s00366-020-01144-2.
Al-Furjan, M., Habibi, M., won Jung, D., Chen, G., Safarpour, M. and Safarpour, H. (2020), "Chaotic responses and nonlinear dynamics of the graphene nanoplatelets reinforced doubly-curved panel", *Europ. J. Mech.-A/Solids*. 104091. https://doi.org/10.1016/j.euromechsol.2020.104091.
Al-Furjan, M., Habibi, M., Won Jung, D., Sadeghi, S., Safarpour, H., Tounsi, A. and Chen, G. (2020), "A computational framework for propagated waves in a sandwich doubly curved nanocomposite panel", *Eng. Comput*., 1-18. https://doi.org/10.1007/s00366-020-01130-8.
Al-Furjan, M., Mohammadgholiha, M., Alarifi, I.M., Habibi, M. and Safarpour, H. (2020), "On the phase velocity simulation of the multi curved viscoelastic system via an exact solution framework", *Eng. Comput*., 1-17. https://doi.org/10.1007/s00366-020-01152-2
Al-Furjan, M., Oyarhossein, M.A., Habibi, M., Safarpour, H. and Jung, D.W. (2020), "Frequency and critical angular velocity characteristics of rotary laminated cantilever microdisk via two-dimensional analysis", *Thin-Walled Struct*., **157**, 107111. https://doi.org/10.1016/j.tws.2020.107111.
Al-Furjan, M., Oyarhossein, M.A., Habibi, M., Safarpour, H. and Jung, D.W. (2020), "Wave propagation simulation in an electrically open shell reinforced with multi-phase nanocomposites", *Eng. Comput*., 1-17. https://doi.org/10.1007/s00366-020-01167-9.
Al-Furjan, M., Oyarhossein, M.A., Habibi, M., Safarpour, H., Jung, D.W. and Tounsi, A. (2020), "On the wave propagation of the multi-scale hybrid nanocomposite doubly curved viscoelastic panel", *Compos. Struct*., 112947. https://doi.org/10.1016/j.compstruct.2020.112947.
Al-Furjan, M., Safarpour, H., Habibi, M., Safarpour, M. and Tounsi, A. (2020), "A comprehensive computational approach for nonlinear thermal instability of the electrically FG-GPLRC disk based on GDQ method", *Eng. Comput*., 1-18. https://doi.org/10.1007/s00366-020-01088-7.
Alimirzaei, S., Mohammadimehr, M. and Tounsi, A. (2019), "Nonlinear analysis of viscoelastic micro-composite beam with geometrical imperfection using FEM: MSGT electro-magneto-elastic bending, buckling and vibration solutions", *Struct. Eng. Mech*., **71**(5), 485-502. https://doi.org/10.12989/sem.2019.71.5.485.
Asghar, S., Naeem, M.N., Hussain, M., Taj, M. and Tounsi, A. (2020), "Prediction and assessment of nonlocal natural frequencies of DWCNTs: Vibration analysis", *Comput. Concrete*. **25**(2), 133-144. https://doi.org/10.12989/cac.2020.25.2.133.
Atanasov, M.S., Karličić, D. and Kozić, P. (2017), "Forced transverse vibrations of an elastically connected nonlocal orthotropic double-nanoplate system subjected to an in-plane magnetic field", *Acta Mechanica*. **228**(6), 2165-2185. https://doi.org/10.1007/s00707-017-1815-6.
Balubaid, M., Tounsi, A., Dakhel, B. and Mahmoud, S. (2019), "Free vibration investigation of FG nanoscale plate using nonlocal two variables integral refined plate theory", *Comput. Concrete*. **24**(6), 579-586. https://doi.org/10.12989/cac.2019.24.6.579
Barati, M.R. (2018), "A general nonlocal stress-strain gradient theory for forced vibration analysis of heterogeneous porous nanoplates", *Europ. J. Mech.-A/Solids*. **67**, 215-230. https://doi.org/10.1080/15376494.2018.1444235.
Barooti, M.M., Safarpour, H. and Ghadiri, M. (2017), "Critical speed and free vibration analysis of spinning 3D single-walled carbon nanotubes resting on elastic foundations", *Europ. Phys. J. Plus*. **132**(1), https://doi.org/10.1140/epjp/i2017-11275-5.
Barretta, R., Čanađija, M., Luciano, R. and de Sciarra, F.M. (2018), "Stress-driven modeling of nonlocal thermoelastic behavior of nanobeams", *Int. J. Eng. Sci*., **126**, 53-67. https://doi.org/10.1016/j.ijengsci.2018.02.012.
Barretta, R., Luciano, R. and Marotti de Sciarra, F. (2015), "A fully gradient model for Euler-Bernoulli nanobeams", *Mathem. Prob. Eng*., **2015**, https://doi.org/10.1155/2015/495095.
Bedia, W.A., Houari, M.S.A., Bessaim, A., Bousahla, A.A., Tounsi, A., Saeed, T. and Alhodaly, M.S. (2019). "A new hyperbolic two-unknown beam model for bending and buckling analysis of a nonlocal strain gradient nanobeams", *J. Nano Res.*, https://doi.org/10.4028/www.scientific.net/JNanoR.57.175.
Belbachir, N., Draich, K., Bousahla, A.A., Bourada, M., Tounsi, A. and Mohammadimehr, M. (2019), "Bending analysis of anti-symmetric cross-ply laminated plates under nonlinear thermal and mechanical loadings", *Steel Compos. Struct*., **33**(1), 81-92. https://doi.org/10.12989/scs.2019.33.1.081.
Bellal, M., Hebali, H., Heireche, H., Bousahla, A.A., Tounsi, A., Bourada, F., Mahmoud, S., Bedia, E. and Tounsi, A. (2020), "Buckling behavior of a single-layered graphene sheet resting on viscoelastic medium via nonlocal four-unknown integral model", *Steel Compos. Struct*., **34**(5), 643-655. https://doi.org/10.12989/scs.2020.34.5.643.
Berghouti, H., Adda Bedia, E., Benkhedda, A. and Tounsi, A. (2019), "Vibration analysis of nonlocal porous nanobeams made of functionally graded material", *Advan. Nano Res*., **7**(5), 351-364. https://doi.org/10.12989/anr.2019.7.5.351.
Boulefrakh, L., Hebali, H., Chikh, A., Bousahla, A.A., Tounsi, A. and Mahmoud, S. (2019), "The effect of parameters of visco-Pasternak foundation on the bending and vibration properties of a thick FG plate", *Geomech. Eng*., **18**(2), 161-178. https://doi.org/10.12989/gae.2019.18.2.161.
Bourada, F., Bousahla, A.A., Tounsi, A., Bedia, E., Mahmoud, S., Benrahou, K.H. and Tounsi, A. (2020), "Stability and dynamic analyses of SW-CNT reinforced concrete beam resting on

elastic-foundation", *Comput. Concrete*. **25**(6), 485-495. https://doi.org/10.12989/cac.2020.25.6.485.

Bousahla, A.A., Bourada, F., Mahmoud, S., Tounsi, A., Algarni, A., Bedia, E. and Tounsi, A. (2020), "Buckling and dynamic behavior of the simply supported CNT-RC beams using an integral-first shear deformation theory", *Comput. Concrete*. **25**(2), 155-166. https://doi.org/10.12989/cac.2020.25.2.155.

Boussoula, A., Boucham, B., Bourada, M., Bourada, F., Tounsi, A., Bousahla, A.A. and Tounsi, A. (2020), "A simple nth-order shear deformation theory for thermomechanical bending analysis of different configurations of FG sandwich plates", *Smart Struct. Syst*., **25**(2), 197-218. https://doi.org/10.12989/sss.2020.25.2.197.

Boutaleb, S., Benrahou, K.H., Bakora, A., Algarni, A., Bousahla, A.A., Tounsi, A., Tounsi, A. and Mahmoud, S. (2019), "Dynamic analysis of nanosize FG rectangular plates based on simple nonlocal quasi 3D HSDT", *Advan. Nano Res*., **7**(3), 191. https://doi.org/10.12989/anr.2019.7.3.191.

Čanađija, M., Barretta, R. and De Sciarra, F.M. (2016), "A gradient elasticity model of Bernoulli–Euler nanobeams in non-isothermal environments", *Europ. J. Mecha.-A/Solids*. **55**, 243-255. https://doi.org/10.1016/j.euromechsol.2015.09.008.

Chen, D., Kitipornchai, S. and Yang, J. (2016), "Nonlinear free vibration of shear deformable sandwich beam with a functionally graded porous core", *Thin-Walled Struct.*, **107**, 39-48. https://doi.org/10.1016/j.tws.2016.05.025.

Chen, S., Hassanzadeh-Aghdam, M. and Ansari, R. (2018), "An analytical model for elastic modulus calculation of SiC whisker-reinforced hybrid metal matrix nanocomposite containing SiC nanoparticles", *J. Alloys Compounds*. **767**, 632-641. https://doi.org/10.1016/j.jallcom.2018.07.102.

Chen, Y., He, L., Guan, Y., Lu, H. and Li, J. (2017), "Life cycle assessment of greenhouse gas emissions and water-energy optimization for shale gas supply chain planning based on multi-level approach: Case study in Barnett, Marcellus, Fayetteville, and Haynesville shales", *Energy Convers. Managem*., **134**, 382-398. https://doi.org/10.1016/j.enconman.2016.12.019.

Chikr, S.C., Kaci, A., Bousahla, A.A., Bourada, F., Tounsi, A., Bedia, E., Mahmoud, S., Benrahou, K.H. and Tounsi, A. (2020), "A novel four-unknown integral model for buckling response of FG sandwich plates resting on elastic foundations under various boundary conditions using Galerkin's approach", *Geomech. Eng*., **21**(5), 471-487. https://doi.org/10.12989/gae.2020.21.5.471.

Dong, Y., He, L., Wang, L., Li, Y. and Yang, J. (2018), "Buckling of spinning functionally graded graphene reinforced porous nanocomposite cylindrical shells: an analytical study", *Aerosp. Sci. Technol*., **82**, 466-478. https://doi.org/10.1016/j.ast.2018.09.037.

Dong, Y., Li, X., Gao, K., Li, Y. and Yang, J. (2020), "Harmonic resonances of graphene-reinforced nonlinear cylindrical shells: effects of spinning motion and thermal environment", *Nonlinear. Dyn.*. **99**(2), 981-1000. https://doi.org/10.1007/s11071-019-05297-8.

Dong, Y., Zhu, B., Wang, Y., He, L., Li, Y. and Yang, J. (2019), "Analytical prediction of the impact response of graphene reinforced spinning cylindrical shells under axial and thermal loads", *Appl. Mathem. Modelling*. **71**, 331-348. https://doi.org/10.1016/j.apm.2019.02.024.

Dong, Y., Zhu, B., Wang, Y., Li, Y. and Yang, J. (2018), "Nonlinear free vibration of graded graphene reinforced cylindrical shells: Effects of spinning motion and axial load", *J. Sound Vib*., **437**, 79-96. https://doi.org/10.1016/j.jsv.2018.08.036.

Draoui, A., Zidour, M., Tounsi, A. and Adim, B. (2019), "Static and dynamic behavior of nanotubes-reinforced sandwich plates using (FSDT)", *J. Nano Res.*, https://doi.org/10.4028/www.scientific.net/JNanoR.57.117.

Du, C., Li, Y. and Jin, X. (2014), "Nonlinear forced vibration of functionally graded cylindrical thin shells", *Thin-Walled Struct*., **78**, 26-36. https://doi.org/10.1016/j.tws.2013.12.010.

Ebrahimi, F., Supeni, E.E.B., Habibi, M. and Safarpour, H. (2020), "Frequency characteristics of a GPL-reinforced composite microdisk coupled with a piezoelectric layer", *Europ. Phys. J. Plus*. **135**(2), 144. https://doi.org/10.1140/epjp/s13360-020-00217-x.

El-Hassar, S.M., Benyoucef, S., Heireche, H. and Tounsi, A. (2016), "Thermal stability analysis of solar functionally graded plates on elastic foundation using an efficient hyperbolic shear deformation theory", *Geomech. Eng*., **10**(3), 357-386. https://doi.org/10.12989/gae.2016.10.3.357.

Fahsi, A., Tounsi, A., Hebali, H., Chikh, A., Adda Bedia, E. and Mahmoud, S. (2017), "A four variable refined nth-order shear deformation theory for mechanical and thermal buckling analysis of functionally graded plates", *Geomech. Eng*., **13**(3), 385-410. https://doi.org/10.12989/gae.2017.13.3.385.

Feng, C., Kitipornchai, S. and Yang, J. (2017), "Nonlinear bending of polymer nanocomposite beams reinforced with non-uniformly distributed graphene platelets (GPLs)", *Compos. Part B: Eng*., **110**, 132-140. https://doi.org/10.1016/j.compositesb.2016.11.024.

Gao, N., Hou, H. and Wu, J.H. (2018), "A composite and deformable honeycomb acoustic metamaterial", *Int. J. Modern Phys. B*. **32**(20), 1850204. https://doi.org/10.1142/S0217979218502041.

Gao, N., Luo, D., Cheng, B. and Hou, H. (2020), "Teaching-learning-based optimization of a composite metastructure in the 0–10 kHz broadband sound absorption range", *J. Acoustic. Soc. Amer*., **148**(2), EL125-EL129. https://doi.org/10.1121/10.0001678.

Gao, N., Tang, L., Deng, J., Lu, K., Hou, H. and Chen, K. "Design, fabrication and sound absorption test of composite porous metamaterial with embedding I-plates into porous polyurethane sponge", *Appl. Acoustic*., **175**, 107845. https://doi.org/10.1016/j.apacoust.2020.107845.

Gao, N., Wei, Z., Zhang, R. and Hou, H. (2019), "Low-frequency elastic wave attenuation in a composite acoustic black hole beam", *Appl. Acoustics*. **154**, 68-76. https://doi.org/10.1016/j.apacoust.2019.04.029

Gao, N., Wu, J., Lu, K. and Zhong, H. "Hybrid composite meta-porous structure for improving and broadening sound absorption", *Mech. Syst. Signal Processing*. **154**, 107504. https://doi.org/10.1016/j.ymssp.2020.107504.

Gao, N., Wu, J.H., Yu, L. and Hou, H. (2016), "Ultralow frequency acoustic bandgap and vibration energy recovery in tetragonal folding beam phononic crystal", *Int. J. Modern Phys. B*. **30**(18), 1650111. https://doi.org/10.1142/S0217979216501113.

Ghabussi, A., Ashrafi, N., Shavalipour, A., Hosseinpour, A., Habibi, M., Moayedi, H., Babaei, B. and Safarpour, H. (2019), "Free vibration analysis of an electro-elastic GPLRC cylindrical shell surrounded by viscoelastic foundation using modified length-couple stress parameter", *Mech. Based Des. Struct. Mach*., 1-25. https://doi.org/10.1080/15397734.2019.1705166.

Habibi, M., Mohammadi, A., Safarpour, H., Shavalipour, A. and Ghadiri, M. (2019), "Wave propagation analysis of the laminated cylindrical nanoshell coupled with a piezoelectric actuator", *Mechanics Based Design of Structures and Machines*. 1-19. https://doi.org/10.1080/15397734.2019.1697932

Habibi, M., Safarpour, M. and Safarpour, H. (2020), "Vibrational characteristics of a FG-GPLRC viscoelastic thick annular plate using fourth-order Runge-Kutta and GDQ methods", *Mech. Based Des. Struct. Mach*., 1-22.

https://doi.org/10.1080/15397734.2020.1779086.

He, L., Chen, Y. and Li, J. (2018), "A three-level framework for balancing the tradeoffs among the energy, water, and air-emission implications within the life-cycle shale gas supply chains", *Resour., Conserv. Recy.*, **133**, 206-228. https://doi.org/10.1016/j.resconrec.2018.02.015.

He, L., Chen, Y., Zhao, H., Tian, P., Xue, Y. and Chen, L. (2018), "Game-based analysis of energy-water nexus for identifying environmental impacts during Shale gas operations under stochastic input", *Sci. Total Environ.*, **627**, 1585-1601. https://doi.org/10.1016/j.scitotenv.2018.02.004.

He, L., Liu, J., Liu, Y., Cui, B., Hu, B., Wang, M., Tian, K., Song, Y., Wu, S. and Zhang, Z. (2019), "Titanium dioxide encapsulated carbon-nitride nanosheets derived from MXene and melamine-cyanuric acid composite as a multifunctional electrocatalyst for hydrogen and oxygen evolution reaction and oxygen reduction reaction", *Appl. Catalysis B: Environment.*, **248**, 366-379. https://doi.org/10.1016/j.apcatb.2019.02.033.

Hellal, H., Bourada, M., Hebali, H., Bourada, F., Tounsi, A., Bousahla, A.A. and Mahmoud, S. (2019), "Dynamic and stability analysis of functionally graded material sandwich plates in hygro-thermal environment using a simple higher shear deformation theory", *J. Sandwich Struct. Mater.*, 1099636219845841. https://doi.org/10.1177/1099636219845841.

Hussain, M., Naeem, M.N., Taj, M. and Tounsi, A. (2020), "Simulating vibration of single-walled carbon nanotube using Rayleigh-Ritz's method", *Advan. Nano Res.*, **8**(3), 215-228. https://doi.org/10.12989/anr.2020.8.3.215.

Hussain, M., Naeem, M.N., Tounsi, A. and Taj, M. (2019), "Nonlocal effect on the vibration of armchair and zigzag SWCNTs with bending rigidity", *Advan. Nano Res.*, **7**(6), 431-442. https://doi.org/10.12989/anr.2019.7.6.431.

Issad, M.N., Fekrar, A., Bakora, A., Bessaim, A. and Tounsi, A. (2018), "Free vibration and buckling analysis of orthotropic plates using a new two variable refined plate theory", *Geomech. Eng.*, **15**(1), 711-719. https://doi.org/10.12989/gae.2018.15.1.711.

Karami, B., Janghorban, M. and Tounsi, A. (2019), "Galerkin's approach for buckling analysis of functionally graded anisotropic nanoplates/different boundary conditions", *Eng. Comput.*, **35**(4), 1297-1316. https://doi.org/10.1007/s00366-018-0664-9.

Li, X., Qin, Y., Li, Y. and Zhao, X. (2018), "The coupled vibration characteristics of a spinning and axially moving composite thin-walled beam", *Mech. Advan. Mater. Struct.*, **25**(9), 722-731. https://doi.org/10.1080/15376494.2017.1308598.

Li, Z., Zhou, H., Hu, D. and Zhang, C. (2020), "Yield criterion for rocklike geomaterials based on strain energy and CMP model", *Int. J. Geomech.*, **20**(3), 04020013. https://doi.org/10.1061/(ASCE)GM.1943-5622.0001593.

Lin, J., Hu, J., Wang, W., Liu, K., Zhou, C., Liu, Z., Kong, S., Lin, S., Deng, Y. and Guo, Z. (2020), "Thermo and light-responsive strategies of smart titanium-containing composite material surface for enhancing bacterially anti-adhesive property", *Chem. Eng. J.*, 125783. https://doi.org/10.1016/j.cej.2020.125783.

Liu, J., Liu, Y. and Wang, X. (2020), "An environmental assessment model of construction and demolition waste based on system dynamics: a case study in Guangzhou", *Environm. Sci. Pollut. Res.*, **27**(30), 37237-37259. https://doi.org/10.1007/s11356-019-07107-5.

Liu, Y., Hu, B., Wu, S., Wang, M., Zhang, Z., Cui, B., He, L. and Du, M. (2019), "Hierarchical nanocomposite electrocatalyst of bimetallic zeolitic imidazolate framework and MoS2 sheets for non-Pt methanol oxidation and water splitting", *Appl. Catalysis B: Environ.*, **258**, 117970. https://doi.org/10.1016/j.apcatb.2019.117970.

Lu, H., Tian, P. and He, L. (2019), "Evaluating the global potential of aquifer thermal energy storage and determining the potential worldwide hotspots driven by socio-economic, geo-hydrologic and climatic conditions", *Renew. Sustain. Energy Rev.*, **112,** 788-796. https://doi.org/10.1016/j.rser.2019.06.013.

Luo, X., Guo, J., Chang, P., Qian, H., Pei, F., Wang, W., Miao, K., Guo, S. and Feng, G. (2020), "ZSM-5@ MCM-41 composite porous materials with a core-shell structure: Adjustment of mesoporous orientation basing on interfacial electrostatic interactions and their application in selective aromatics transport", *Separation Purification Technol.*, **239**, 116516. https://doi.org/10.1016/j.seppur.2020.116516.

Lv, Q., Liu, H., Wang, J., Liu, H. and Shang, Y. (2020), "Multiscale analysis on spatiotemporal dynamics of energy consumption CO2 emissions in China: Utilizing the integrated of DMSP-OLS and NPP-VIIRS nighttime light datasets", *Sci. Total Environ.*, **703**, 134394. https://doi.org/10.1016/j.scitotenv.2019.134394.

Mahmoudi, A., Benyoucef, S., Tounsi, A., Benachour, A., Adda Bedia, E.A. and Mahmoud, S. (2019), "A refined quasi-3D shear deformation theory for thermo-mechanical behavior of functionally graded sandwich plates on elastic foundations", *J. Sandwich Struct. Mater.*, **21**(6), 1906-1929. https://doi.org/10.1177/1099636217727577.

Matouk, H., Bousahla, A.A., Heireche, H., Bourada, F., Bedia, E., Tounsi, A., Mahmoud, S., Tounsi, A. and Benrahou, K. (2020), "Investigation on hygro-thermal vibration of P-FG and symmetric S-FG nanobeam using integral Timoshenko beam theory", *Advan. Nano Res.*, **8**(4), 293-305. https://doi.org/10.12989/anr.2020.8.4.293.

Medani, M., Benahmed, A., Zidour, M., Heireche, H., Tounsi, A., Bousahla, A.A., Tounsi, A. and Mahmoud, S. (2019), "Static and dynamic behavior of (FG-CNT) reinforced porous sandwich plate using energy principle", *Steel Compos. Struct.*, **32**(5), 595-610. https://doi.org/10.12989/scs.2019.32.5.595.

Mirsalehi, M., Azhari, M. and Amoushahi, H. (2017), "Buckling and free vibration of the FGM thin micro-plate based on the modified strain gradient theory and the spline finite strip method", *Europ. J. Mech.-A/Solids*. **61**, 1-13. https://doi.org/10.1016/j.euromechsol.2016.08.008.

Moayedi, H., Aliakbarlou, H., Jebeli, M., Noormohammadiarani, O., Habibi, M., Safarpour, H. and Foong, L. (2020), "Thermal buckling responses of a graphene reinforced composite micropanel structure", *Int. J. Appl. Mech.*, **12**(01), 2050010. https://doi.org/10.1142/S1758825120500106.

Moayedi, H., Darabi, R., Ghabussi, A., Habibi, M. and Foong, L.K. (2020), "Weld orientation effects on the formability of tailor welded thin steel sheets", *Thin-Wall. Struct.*, **149**, 106669. https://doi.org/10.1016/j.tws.2020.106669.

Oyarhossein, M.A., Alizadeh, A.A., Habibi, M., Makkiabadi, M., Daman, M., Safarpour, H. and Jung, D.W. (2020), "Dynamic response of the nonlocal strain-stress gradient in laminated polymer composites microtubes", *Sci. Reports*. **10**(1), 1-19. https://doi.org/10.1038/s41598-020-61855-w.

Pellicano, F. (2007), "Vibrations of circular cylindrical shells: theory and experiments", *J. Sound Vib.*, **303**(1-2), 154-170. https://doi.org/10.1016/j.jsv.2007.01.022.

Rabhi, M., Benrahou, K.H., Kaci, A., Houari, M.S.A., Bourada, F., Bousahla, A.A., Tounsi, A., Bedia, E.A., Mahmoud, S. and Tounsi, A. (2020), "A new innovative 3-unknowns HSDT for buckling and free vibration of exponentially graded sandwich plates resting on elastic foundations under various boundary conditions", *Geomech. Eng.*, **22**(2), 119. https://doi.org/10.12989/gae.2020.22.2.119.

Rafiee, M.A., Rafiee, J., Wang, Z., Song, H., Yu, Z.Z. and Koratkar, N. (2009), "Enhanced mechanical properties of

nanocomposites at low graphene content", *ACS Nano*, **3**(12), 3884-3890. https://doi.org/10.1021/nn9010472.

Refrafi, S., Bousahla, A.A., Bouhadra, A., Menasria, A., Bourada, F., Tounsi, A., Bedia, E., Mahmoud, S., Benrahou, K.H. and Tounsi, A. (2020), "Effects of hygro-thermo-mechanical conditions on the buckling of FG sandwich plates resting on elastic foundations", *Comput. Concrete*. **25**(4), 311-325. https://doi.org/10.12989/cac.2020.25.4.311.

Sadoun, M., Houari, M.S.A., Bakora, A., Tounsi, A., Mahmoud, S. and Alwabli, A.S. (2018), "Vibration analysis of thick orthotropic plates using quasi 3D sinusoidal shear deformation theory", *Geomech. Eng*., **16**(2), 141-150. https://doi.org/10.12989/gae.2018.16.2.141.

Safarpour, M., Ghabussi, A., Ebrahimi, F., Habibi, M. and Safarpour, H. (2020), "Frequency characteristics of FG-GPLRC viscoelastic thick annular plate with the aid of GDQM", *Thin-Wall. Struct*., **150**, 106683. https://doi.org/10.1016/j.tws.2020.106683.

Sahmani, S. and Aghdam, M. (2017), "A nonlocal strain gradient hyperbolic shear deformable shell model for radial postbuckling analysis of functionally graded multilayer GPLRC nanoshells", *Compos. Struct*., **178**, 97-109. https://doi.org/10.1016/j.compstruct.2017.06.062.

Sahmani, S. and Aghdam, M. (2017), "Nonlinear instability of axially loaded functionally graded multilayer graphene platelet-reinforced nanoshells based on nonlocal strain gradient elasticity theory", *Int. J. Mech. Sci*., **131**, 95-106. https://doi.org/10.1016/j.ijmecsci.2017.06.052.

Sahmani, S., Aghdam, M.M. and Rabczuk, T. (2018), "Nonlocal strain gradient plate model for nonlinear large-amplitude vibrations of functionally graded porous micro/nano-plates reinforced with GPLs", *Compos. Struct*., **198**, 51-62. https://doi.org/10.1016/j.compstruct.2018.05.031.

Semmah, A., Heireche, H., Bousahla, A.A. and Tounsi, A. (2019), "Thermal buckling analysis of SWBNNT on Winkler foundation by non local FSDT", *Advan. Nano Res*., **7**(2), 89. https://doi.org/10.12989/anr.2019.7.2.089.

Shafiei, N., Mirjavadi, S.S., Afshari, B.M., Rabby, S. and Hamouda, A. (2017), "Nonlinear thermal buckling of axially functionally graded micro and nanobeams", *Compos. Struct*., **168**, 428-439. https://doi.org/10.1016/j.compstruct.2017.02.048.

Shahsiah, R. and Eslami, M. (2003), "Thermal buckling of functionally graded cylindrical shell", *J. Therm. Stresses*. **26**(3), 277-294. https://doi.org/10.1080/713855892.

Shi, G., Araby, S., Gibson, C.T., Meng, Q., Zhu, S. and Ma, J. (2018), "Graphene platelets and their polymer composites: fabrication, structure, properties, and applications", *Advan. Funct. Mater*., **28**(19), 1706705. https://doi.org/10.1002/adfm.201706705.

Shi, M., Narayanasamy, M., Yang, C., Zhao, L., Jiang, J., Angaiah, S. and Yan, C. (2020), "3D interpenetrating assembly of partially oxidized MXene confined Mn–Fe bimetallic oxide for superior energy storage in ionic liquid", *Electrochimica Acta*. **334**, 135546. https://doi.org/10.1016/j.electacta.2019.135546.

Shi, M., Xiao, P., Lang, J., Yan, C. and Yan, X. (2020), "Porous g-C3N4 and MXene dual-confined FeOOH quantum dots for superior energy storage in an ionic liquid", *Advan. Science*. **7**(2), 1901975. https://doi.org/10.1002/advs.201901975.

Shokrgozar, A., Ghabussi, A., Ebrahimi, F., Habibi, M. and Safarpour, H. (2020), "Viscoelastic dynamics and static responses of a graphene nanoplatelets-reinforced composite cylindrical microshell", *Mech. Based Des. Struct. Mach*., 1-28. https://doi.org/10.1080/15397734.2020.1719509.

Song, M., Kitipornchai, S. and Yang, J. (2017), "Free and forced vibrations of functionally graded polymer composite plates reinforced with graphene nanoplatelets", *Compos. Struct*., **159**, 579-588. https://doi.org/10.1016/j.compstruct.2016.09.070.

Tadi Beni, Y., Mehralian, F. and Zeighampour, H. (2016), "The modified couple stress functionally graded cylindrical thin shell formulation", *Mech. Advan. Mater. Struct*., **23**(7), 791-801. https://doi.org/10.1080/15376494.2015.1029167.

Tounsi, A., Al-Dulaijan, S., Al-Osta, M.A., Chikh, A., Al-Zahrani, M., Sharif, A. and Tounsi, A. (2020), "A four variable trigonometric integral plate theory for hygro-thermo-mechanical bending analysis of AFG ceramic-metal plates resting on a two-parameter elastic foundation", *Steel Compos. Struct*., **34**(4), 511-524. https://doi.org/10.12989/scs.2020.34.4.511.

Wang, B., Zhang, L., Ma, H., Wang, H. and Wan, S. (2019), "Parallel LSTM-based regional integrated energy system multienergy source-load information interactive energy prediction", *Complexity*. **2019**. https://doi.org/10.1155/2019/7414318.

Wang, J., Huang, Y., Wang, T., Zhang, C. and hui Liu, Y. (2020), "Fuzzy finite-time stable compensation control for a building structural vibration system with actuator failures", *Appl. Soft Comput*., 106372. ttps://doi.org/10.1016/j.asoc.2020.106372.

Wang, M., Guo, Y., Wang, B., Luo, H., Zhang, X., Wang, Q., Zhang, Y., Wu, H., Liu, H. and Dou, S. (2020), "An engineered self-supported electrocatalytic cathode and dendrite-free composite anode based on 3D double-carbon hosts for advanced Li–SeS 2 batteries", *J. Mater. Chemistry A*. **8**(6), 2969-2983.

Wang, P., Yao, T., Li, Z., Wei, W., Xie, Q., Duan, W. and Han, H. (2020), "A superhydrophobic/electrothermal synergistically anti-icing strategy based on graphene composite", *Compos. Sci. Technol*., **198**, 108307. https://doi.org/10.1016/j.compscitech.2020.108307.

Wang, Y., Feng, C., Santiuste, C., Zhao, Z. and Yang, J. (2019), "Buckling and postbuckling of dielectric composite beam reinforced with Graphene Platelets (GPLs)", *Aerosp. Sci. Technol*., **91**, 208-218. https://doi.org/10.1016/j.ast.2019.05.008.

Wang, Y., Yao, M., Ma, R., Yuan, Q., Yang, D., Cui, B., Ma, C., Liu, M. and Hu, D. (2020), "Design strategy of barium titanate/polyvinylidene fluoride-based nanocomposite films for high energy storage", *J. Mater. Chemistry A*. **8**(3), 884-917. https://doi.org/10.1039/C9TA11527G.

Wu, H., Kitipornchai, S. and Yang, J. (2017), "Thermal buckling and postbuckling of functionally graded graphene nanocomposite plates", *Mater. Des*., **132**, 430-441. https://doi.org/10.1016/j.matdes.2017.07.025.

Xu, H.B., Zhang, C.W., Li, H., Tan, P., Ou, J.P. and Zhou, F.L. (2014), "Active mass driver control system for suppressing wind-induced vibration of the Canton Tower", *Smart Struct. Syst*., **13**(2), 281-303. https://doi.org/10.12989/sss.2014.13.2.281.

Yang, C., Gao, F. and Dong, M. (2020), "Energy efficiency modeling of integrated energy system in coastal areas", *J. Coastal Res*., **103**(SI), 995-1001. https://doi.org/10.2112/SI103-207.1.

Yang, J., Chen, D. and Kitipornchai, S. (2018), "Buckling and free vibration analyses of functionally graded graphene reinforced porous nanocomposite plates based on Chebyshev-Ritz method", *Compos. Struct*., **193**, 281-294. https://doi.org/10.1016/j.compstruct.2018.03.090.

Yang, Z., Xu, P., Wei, W., Gao, G., Zhou, N. and Wu, G. (2020), "Influence of the crosswind on the pantograph arcing dynamics", *IEEE Transactions Plasma Sci*., **48**(8), 2822-2830. https://doi.org/10.1109/TPS.2020.3010553.

Yavari, F., Rafiee, M., Rafiee, J., Yu, Z.Z. and Koratkar, N. (2010), "Dramatic increase in fatigue life in hierarchical graphene composites", *ACS Appl. Mater. Interfaces*. **2**(10), 2738-2743. https://doi.org/10.1021/am100728r.

Younsi, A., Tounsi, A., Zaoui, F.Z., Bousahla, A.A. and

Mahmoud, S. (2018), "Novel quasi-3D and 2D shear deformation theories for bending and free vibration analysis of FGM plates", *Geomech. Eng.*, **14**(6), 519-532. https://doi.org/10.12989/gae.2018.14.6.519.

Yu, D., Mao, Y., Gu, B., Nojavan, S., Jermsittiparsert, K. and Nasseri, M. (2020), "A new LQG optimal control strategy applied on a hybrid wind turbine/solid oxide fuel cell/in the presence of the interval uncertainties", *Sustain. Energy, Grids Networks*. **21**, 100296. https://doi.org/10.1016/j.segan.2019.100296.

Zarga, D., Tounsi, A., Bousahla, A.A., Bourada, F. and Mahmoud, S. (2019), "Thermomechanical bending study for functionally graded sandwich plates using a simple quasi-3D shear deformation theory", *Steel Compos. Struct.*, **32**(3), 389-410. https://doi.org/10.12989/scs.2019.32.3.389.

Zhang, C. (2014), "Control force characteristics of different control strategies for the wind-excited 76-story benchmark building structure", *Advan. Struct. Eng.*, **17**(4), 543-559. https://doi.org/10.1260/1369-4332.17.4.543.

Zhang, C. and Ou, J. (2008), "Control structure interaction of electromagnetic mass damper system for structural vibration control", *J. Eng. Mech.*, **134**(5), 428-437. https://doi.org/10.1061/(ASCE)0733-9399(2008)134:5(428).

Zhang, C. and Ou, J. (2015), "Modeling and dynamical performance of the electromagnetic mass driver system for structural vibration control", *Eng. Struct.*, **82**, 93-103. https://doi.org/10.1016/j.engstruct.2014.10.029.

Zhang, C. and Wang, H. (2019), "Robustness of the active rotary inertia driver system for structural swing vibration control subjected to multi-type hazard excitations", *Appl. Sci.*, **9**(20), 4391. https://doi.org/10.3390/app9204391.

Zhang, C. and Wang, H. (2020), "Swing vibration control of suspended structures using the Active Rotary Inertia Driver system: Theoretical modeling and experimental verification", *Struct. Control Health Monit.*, **27**(6), e2543. https://doi.org/10.1002/stc.2543.

Zhang, S., Pak, R.Y. and Zhang, J. (2020), "Vertical time-harmonic coupling vibration of an impermeable, rigid, circular plate resting on a finite, poroelastic soil layer", *Acta Geotechnica*. 1-25. https://doi.org/10.1007/s11440-020-01067-8.

Zhang, W. (2020), "Parameter Adjustment Strategy and Experimental Development of Hydraulic System for Wave Energy Power Generation", *Symmetry.* **12**(5), 711. https://doi.org/10.3390/sym12050711.

Zhao, S., Zhao, Z., Yang, Z., Ke, L., Kitipornchai, S. and Yang, J. (2020), "Functionally graded graphene reinforced composite structures: A review", *Eng. Struct.*, **210**, 110339. https://doi.org/10.1016/j.engstruct.2020.110339.

Zhao, X., Ye, Y., Ma, J., Shi, P. and Chen, H. (2020), "Construction of electric vehicle driving cycle for studying electric vehicle energy consumption and equivalent emissions", *Environ. Sci. Pollut. Res.*, 1-15. https://doi.org/10.1007/s11356-020-09094-4.

Zhu, L., Kong, L. and Zhang, C. (2020), "Numerical study on hysteretic behaviour of horizontal-connection and energy-dissipation structures developed for prefabricated shear walls", *Appl. Sci.*, **10**(4), 1240. https://doi.org/10.3390/app10041240.

Zhu, L., Zhang, C., Guan, X., Uy, B., Sun, L. and Wang, B. (2018), "The multi-axial strength performance of composited structural BCW members subjected to shear forces", *Steel Compos. Struct.*, **27**(1), 75-87. https://doi.org/10.12989/scs.2018.27.1.075.

Zuo, X., Dong, M., Gao, F. and Tian, S. (2020), "The modeling of the electric heating and cooling system of the integrated energy system in the coastal area", *J. Coast. Res.*, **103**(SI), 1022-1029. https://doi.org/10.2112/SI103-213.1.

CC